
# Beamforming Design for Wireless Information and Power Transfer Systems: Receive Power-Splitting vs Transmit Time-Switching

Nasir, A. A., Tuan, H. D., Duong, T. Q., & Poor, H. V. (2016). Beamforming Design for Wireless Information and Power Transfer Systems: Receive Power-Splitting vs Transmit Time-Switching. *IEEE Transactions on Communications*, *65*(2), 876. https://doi.org/10.1109/TCOMM.2016.2631465

**Published in:**
IEEE Transactions on Communications

**Document Version:**
Peer reviewed version

**Queen's University Belfast - Research Portal:**
Link to publication record in Queen's University Belfast Research Portal

**Publisher rights**
(c) 2016 IEEE. Personal use of this material is permitted. Permission from IEEE must be obtained for all other users, including reprinting/ republishing this material for advertising or promotional purposes, creating new collective works for resale or redistribution to servers or lists, or reuse of any copyrighted components of this work in other works.

**General rights**
Copyright for the publications made accessible via the Queen's University Belfast Research Portal is retained by the author(s) and / or other copyright owners and it is a condition of accessing these publications that users recognise and abide by the legal requirements associated with these rights.

**Take down policy**
The Research Portal is Queen's institutional repository that provides access to Queen's research output. Every effort has been made to ensure that content in the Research Portal does not infringe any person's rights, or applicable UK laws. If you discover content in the Research Portal that you believe breaches copyright or violates any law, please contact openaccess@qub.ac.uk.

Download date:04. May. 2023

# Beamforming Design for Wireless Information and Power Transfer Systems: Receive Power-Splitting vs Transmit Time-Switching

Ali A. Nasir, Hoang D. Tuan, Duy T. Ngo, Trung Q. Duong and H. Vincent Poor

***Abstract*—Information and energy can be transferred over the same radio-frequency channel. In the power-splitting (PS) mode, they are simultaneously transmitted using the same signal by the base station (BS) and later separated at the user (UE)'s receiver by a power splitter. In the time-switching (TS) mode, they are either transmitted separately in time by the BS or received separately in time by the UE. In this paper, the BS transmit beamformers are jointly designed with either the receive PS ratios or the transmit TS ratios in a multicell network that implements wireless information and power transfer (WIPT). Imposing UE harvested energy constraints, the design objectives include (i) maximizing the minimum UE rate under the BS transmit power constraint, and (ii) minimizing the maximum BS transmit power under the UE data rate constraint. New iterative algorithms of low computational complexity are proposed to efficiently solve the formulated difficult nonconvex optimization problems, where each iteration either solves one simple convex quadratic program or one simple second-order-cone-program. Simulation results show that these algorithms converge quickly after only a few iterations. Notably, the transmit TS-based WIPT system is not only more easily implemented but outperforms the receive PS-based WIPT system as it better exploits the beamforming design at the transmitter side.**

***Index Terms*—Energy harvesting, power splitting, quadratic programming, second-order cone programming, time switching, transmit beamforming, wireless information and power transfer**

## I. Introduction

Dense small-cell deployment is identified as one of the 'big pillars' to support the much needed $1,000\times$ increase in data throughput for the fifth-generation (5G) wireless networks [1]. While there is a major concern with the energy consumption of such a dense small-cell deployment, recent advances in wireless power transfer allow the emitted energy in the radio frequency signals to be harvested and recycled [2]–[6]. The scavenged radio frequency (RF) energy is stored in the device battery and later used to power other signal processing and transmitting operations. For example, an radio frequency-powered relay can be opportunistically deployed to extend network coverage without the need to access a main power supply. The wireless power transfer from a base station (BS) to its users (UEs) is viable in a dense small-cell environment, because the close BS-UE proximity enables an adequate amount of radio frequency (RF) energy to be harvested for practical applications [7]–[9].

The two basic realizable receiver structures for separating the received signal for information decoding (ID) and energy harvesting (EH) are power splitting (PS) and time switching (TS) [10]. In the PS approach, information and energy are simultaneously transmitted using the same signal by the BS. At the UE, a power splitter is employed to divide the received signal into two parts of distinct powers, one for ID and another for EH. In the receive TS approach, instead of the power splitter a time switch is applied on the received signal, allowing the UE to decode the information in one portion of time and harvest the energy in the remaining time. In the transmit TS approach, information and energy are transmitted by BS in different portions of time. The UE then processes the received signals for ID and EH separately in time. The TS structure has received considerable research attention (see [3], [11]–[13]) due its simple implementation. Although the performance of the receive TS approach can be worse than the PS approach [3], that of the transmit TS approach has not been reported in the literature.

Transmit beamforming is beneficial for both PS-based and TS-based WIPT systems. With beamforming, the signal beams are steered and the radio frequency (RF) energy is focused at the desired UEs. Beamforming design without energy harvesting has been studied for multicell multi-input-single-output (MISO) [14]–[18] or single-cell MISO [19] networks. Except for [17] and [18], all the formulated problems are solved in a decentralized manner by applying Lagrangian duality and uplink-downlink duality. In a single-cell energy harvesting MISO network with PS-based receivers, [20]–[24] jointly design transmit beamformers at the BS and receive PS ratios at the UEs to minimize the sum beamforming power under UE signal-to-interference-plus-noise-ratio (SINR) and EH constraints. Such indefinite quadratic problem is then recast as a semidefinite program (SDP) with rank-one matrix constraints. The rank-one matrix constraints are dropped to have semidefinite relaxation (SDR) problem.To deal with the rank-more-than-one solution given by SDR, [24] proposes us-

A. A. Nasir is with the Department of Electrical Engineering, King Fahd University of Petroleum and Minerals (KFUPM), Dhahran, Saudi Arabia (Email: anasir@kfupm.edu.sa).

H. D. Tuan is with the Faculty of Engineering and Information Technology, University of Technology Sydney, Broadway, NSW 2007, Australia (email: Tuan.Hoang@uts.edu.au).

D. T. Ngo is with the School of Electrical Engineering and Computing, The University of Newcastle, Callaghan, NSW 2308, Australia (email: duy.ngo@newcastle.edu.au).

T. Q. Duong is with Queen's University Belfast, Belfast BT7 1NN, UK (email: trung.q.duong@qub.ac.uk)

H. V. Poor is with the Department of Electrical Engineering, Princeton University, Princeton, NJ 08544, USA (e-mail: poor@princeton.edu).

This work was supported in part by the U.K. Royal Academy of Engineering Research Fellowship under Grant RF1415\14\22

ing a randomization method after SDR. As shown in [25]–[27], the performance of such a method is inconsistent and could be poor in many cases. An approximate rank-one solution with compromised performance has been proposed in [28]. Suboptimal algorithms based on zero-forcing and maximum ratio transmission are proposed in [21] and [24]. As expected, they are outperformed by the SDR solution. Surprisingly, the joint design of transmit beamformers and TS ratios at the receivers has not been adequately addressed in the literature although it is much easier to practically implement TS-based receivers. The main reason is that even the SDR approach does not lead to solutions with tractable computation in this case. Also to the best of our knowledge, such joint design has not been previously considered for the transmit TS case.

This paper addresses the joint design of transmit beamforming and either PS ratios or transmit TS ratios in a WIPT-enabled MISO multicell network. We choose to investigate the transmit TS approach instead of the receive TS counterpart because of its potential to outperform the receive PS approach. As will be shown later, it is actually the case. Specifically, we consider two important design problems: 1) Maximizing the minimum UE rate under BS transmit power and UE harvested energy constraints, and 2) Minimizing the maximum BS transmit power under the UE rate and harvested energy constraints. As the considered optimization problems are highly nonconvex, their global optimality is not theoretically guaranteed by any practical methods.

Here we exploit the partial convexity structure of the problems to propose new algorithms based on either quadratic programming iteration or second-order cone iteration. Significantly, our simulation results with practical parameters show that the proposed algorithms for the receive PS-based WIPT system tightly approach the bounds provided by the SDR approach. This observation demonstrates their ability to locate the global optimum of the original nonconvex problems in the considered numerical examples. While the upper/lower bound is not available for the transmit TS-based WIPT system by the SDR approach, our practical simulation results reveal that this system outperforms the receive PS-based system due its ability to efficiently exploit the transmit beamforming power. It is worth noting that the TS-based WIPT system is typically simpler to implement than the PS-based counterpart.

The rest of the paper is organized as follows: Section II considers the optimization of the receive PS-based WIPT system whereas Section III considers the optimization of the transmit TS-based WIPT system. Section IV evaluates the performance of our proposed algorithms by numerical examples and analyzes their computational complexity. Finally, Section V concludes the paper.

*Notation*. Standard notation is used throughout the paper. In particular, $\Re\{\cdot\}$ denotes the real part of its argument, $\nabla$ denotes the first-order differential operator, and $\langle \mathbf{x}, \mathbf{y} \rangle \triangleq \mathbf{x}^H \mathbf{y}$.

## II. Max-Min Rate and Min-Max Power Optimization for Receive Power-Splitting WIPT Systems

Consider the downlink of a $K$-cell network. As shown in Fig. 1, the BS of a cell $k \in \mathcal{K} \triangleq \{1, \ldots, K\}$ is equipped

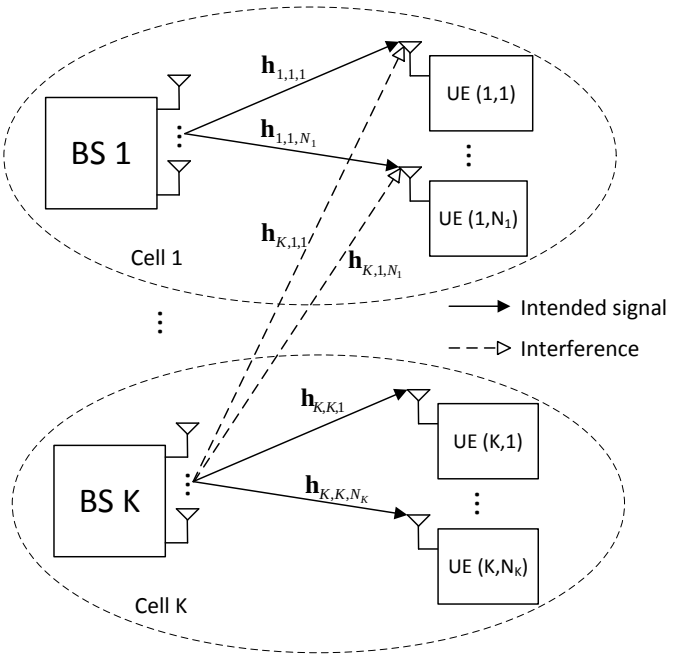


Fig. 1. Downlink multiuser multicell interference scenario consisting of $K$ cells. To keep the drawing clear, we only show the interference scenario in cell 1. In general, the interference occurs in all $K$ cells.

with $M > 1$ antennas and it serves $N_k$ single-antenna UEs within its cell. By BS $k$ and UE $(k, n)$, we mean the BS that serves cell $k$ and the UE $n \in \mathcal{N}_k \triangleq \{1, \ldots, N_k\}$ of the same cell, respectively. Assume universal frequency reuse where all UEs in all cells share the same frequency band. While the radio spectrum is best utilized in this approach, the signal interference situation among multiple UEs in multiple cells is most severe. Beamforming is then used to mitigate the effect of interference by steering the signal beams in the intended directions.

Denote by $\mathbf{w}_{\bar{k},\bar{n}} \in \mathbb{C}^{M\times 1}$ the beamforming vector by BS $\bar{k} \in \mathcal{K}$ for its UE $(\bar{k}, \bar{n})$ where $\bar{n} \in \mathcal{N}_{\bar{k}} \triangleq \{1, \ldots, N_{\bar{k}}\}$. Let $\mathbf{h}_{\bar{k},k,n} \in \mathbb{C}^{M\times 1}$ be the flat fading channel vector between BS $\bar{k}$ and UE $(k, n)$, which includes large-scale pathloss and small-scale fading. Denote $x_{\bar{k},\bar{n}}$ as the information signal to be transmitted by BS $\bar{k}$ to UE $(\bar{k}, \bar{n})$ where $\mathbb{E}\{|x_{\bar{k},\bar{n}}|^2\} = 1$. The complex baseband signal received by UE $(k, n)$ is then expressed as:

$$y_{k,n} = \sum_{\bar{k}\in\mathcal{K}} \mathbf{h}_{\bar{k},k,n}^H \sum_{\bar{n}\in\mathcal{N}_{\bar{k}}} \mathbf{w}_{\bar{k},\bar{n}} x_{\bar{k},\bar{n}} + z_{k,n}^a, \tag{1}$$

where $z_{k,n}^a \sim \mathcal{CN}(0, \sigma_a^2)$ is the zero-mean circularly complex Gaussian noise with variance $\sigma_a^2$ at the receive antenna of UE $(k, n)$. To show the effect of interference at UE $(k, n)$, let us explicitly write (1) as:

$$y_{k,n} = \mathbf{h}_{k,k,n}^H \mathbf{w}_{k,n} x_{k,n} + \mathbf{h}_{k,k,n}^H \sum_{\bar{n}\in\mathcal{N}_k\setminus\{n\}} \mathbf{w}_{k,\bar{n}} x_{k,\bar{n}} + \sum_{\bar{k}\in\mathcal{K}\setminus\{k\}} \mathbf{h}_{\bar{k},k,n}^H \sum_{\bar{n}\in\mathcal{N}_{\bar{k}}} \mathbf{w}_{\bar{k},\bar{n}} x_{\bar{k},\bar{n}} + z_{k,n}^a. \tag{2}$$

The first term in (2) is the intended signal for UE $(n, k)$, the second term is the intracell interference from within cell $k$,

and the third term is the intercell interference from other cells $\bar{k} \in \mathcal{K} \setminus \{k\}$.

The short BS-UE distances allow the UEs to practically implement the wireless information and power transfer. Thus, the UE $(k,n)$ applies the *power splitting* (PS) technique to coordinate both information decoding (ID) and energy harvesting (EH). Specifically, the power splitter divides the received signal $y_{k,n}$ into two parts in the proportion of $\alpha_{k,n} : (1-\alpha_{k,n})$, where $\alpha_{k,n} \in (0,1)$ is termed as the PS ratio for UE $(k,n)$. The first part $\sqrt{\alpha_{k,n}}y_{k,n}$ forms an input to the ID receiver as:

$$\sqrt{\alpha_{k,n}}y_{k,n} + z^c_{k,n} = \sqrt{\alpha_{k,n}}\left(\sum_{\bar{k}\in\mathcal{K}} \mathbf{h}^H_{\bar{k},k,n} \sum_{\bar{n}\in\mathcal{N}_{\bar{k}}} \mathbf{w}_{\bar{k},\bar{n}} x_{\bar{k},\bar{n}} + z^a_{k,n}\right) + z^c_{k,n}, \quad (3)$$

where $z^c_{k,n} \sim \mathcal{CN}(0,\sigma_c^2)$ is the additional noise introduced by the ID receiver circuitry. Upon denoting $\mathbf{w} \triangleq [\mathbf{w}_{k,n}]_{k\in\mathcal{K},n\in\mathcal{N}_k}$ and $\boldsymbol{\alpha} \triangleq [\alpha_{k,n}]_{k\in\mathcal{K},n\in\mathcal{N}_k}$, the signal-to-interference-plus-noise ratio (SINR) at the input of the ID receiver of UE $(k,n)$ is given by:

$$\text{SINR}_{k,n} \triangleq \frac{|\mathbf{h}^H_{k,k,n}\mathbf{w}_{k,n}|^2}{\varphi_{k,n}(\mathbf{w},\alpha_{k,n})}, \quad (4)$$

where

$$\varphi_{k,n}(\mathbf{w},\alpha_{k,n}) \triangleq \underbrace{\sum_{\bar{n}\in\mathcal{N}_k\setminus\{n\}} |\mathbf{h}^H_{k,k,n}\mathbf{w}_{k,\bar{n}}|^2}_{\text{intracell interference}} + \underbrace{\sum_{\bar{k}\in\mathcal{K}\setminus\{k\}}\sum_{\bar{n}\in\mathcal{N}_{\bar{k}}} |\mathbf{h}^H_{\bar{k},k,n}\mathbf{w}_{\bar{k},\bar{n}}|^2}_{\text{intercell interference}} + \sigma_a^2 + \sigma_c^2/\alpha_{k,n},$$

Assuming a normalized time duration of one second, the energy of the second part $\sqrt{1-\alpha_{k,n}}y_{k,n}$ of the received signal $y_{k,n}$ is harvested by the EH receiver of UE $(k,n)$ as

$$E_{k,n}(\mathbf{w},\alpha_{k,n}) \triangleq \zeta_{k,n}(1-\alpha_{k,n})\left(p_{k,n}(\mathbf{w}) + \sigma_a^2\right), \quad (5)$$

where the constant $\zeta_{k,n} \in (0,1)$ denotes the efficiency of energy conversion at the EH receiver,[1] and

$$p_{k,n}(\mathbf{w}) \triangleq \sum_{\bar{k}\in\mathcal{K}}\sum_{\bar{n}\in\mathcal{N}_{\bar{k}}} |\mathbf{h}^H_{\bar{k},k,n}\mathbf{w}_{\bar{k},\bar{n}}|^2.$$

$E_{k,n}$ can be stored in a battery and later used to power the operations of UE $(k,n)$ (e.g., processing the received signals in the downlink, or transmitting data to the BS in the uplink).

### A. Max-Min Rate Iterative Optimization

First, we aim to consider max-min rate optimization problem, which provides fairness in allocating the radio resources to the most disadvantaged user, especially that at the cell edges. As this user suffers from severe interference and only achieves low throughput, it is sensible to maximize its throughput for an acceptable quality of service. We aim to jointly optimize the transmit beamforming vectors $\mathbf{w}_{k,n}$ and the PS ratios $\alpha_{k,n}$ for all $k \in \mathcal{K}$, and $n \in \mathcal{N}_k$ by solving the following max-min rate optimization problem:

$$\max_{\substack{\mathbf{w}_{k,n}\in\mathbb{C}^{M\times 1},\\ \alpha_{k,n}\in(0,1),\\ \forall\, k\in\mathcal{K},\ n\in\mathcal{N}_k}} \min_{k\in\mathcal{K},n\in\mathcal{N}_k} \ln\left(1+\frac{|\mathbf{h}^H_{k,k,n}\mathbf{w}_{k,n}|^2}{\varphi_{k,n}(\mathbf{w},\alpha_{k,n})}\right) \quad (6a)$$

$$\text{s.t.} \quad \sum_{n\in\mathcal{N}_k} \|\mathbf{w}_{k,n}\|^2 \le P_k^{\max},\ \forall k\in\mathcal{K} \quad (6b)$$

$$\sum_{k\in\mathcal{K}}\sum_{n\in\mathcal{N}_k} \|\mathbf{w}_{k,n}\|^2 \le P^{\max}, \quad (6c)$$

$$E_{k,n}(\mathbf{w},\alpha_{k,n}) \ge e^{\min}_{k,n},\ \forall k\in\mathcal{K}, n\in\mathcal{N}_k. \quad (6d)$$

Constraint (6b) caps the total transmit power of each BS $k$ at a predefined value $P_k^{\max}$. Constraint (6c) ensures that the total transmit power of the network will not exceed the allowable budget $P^{\max}$, which helps limit any potential undue interference from the considered multicell network to another network. Constraint (6d) requires that the minimum energy harvested by UE $(k,n)$ exceeds some target $e^{\min}_{k,n}$ for useful EH. It is obvious that (6) is equivalent to the following max-min SINR problem:

$$\max_{\substack{\mathbf{w}_{k,n}\in\mathbb{C}^{M\times 1},\\ \alpha_{k,n}\in(0,1),\\ \forall\ k\in\mathcal{K},\ n\in\mathcal{N}_k}} \min_{k\in\mathcal{K},n\in\mathcal{N}_k} f_{k,n}(\mathbf{w},\alpha_{k,n}) \triangleq \frac{|\mathbf{h}^H_{k,k,n}\mathbf{w}_{k,n}|^2}{\varphi_{k,n}(\mathbf{w},\alpha_{k,n})}$$

$$\text{s.t.} \quad \text{(6b)} - \text{(6d)}. \quad (7)$$

While (6b) and (6c) are convex, the objective in (7) is not concave and the constraint (6d) is not convex due to the strong coupling between $\mathbf{w}_{k,n}$ and $\alpha_{k,n}$ in both the SINR and EH expressions [see (4) and (5)]. Moreover, the objective in (7) is also nonsmooth due to the minimization operator. Indeed, (7) is a nonconvex nonsmooth function optimization problem subject to nonconvex constraints. If one fixes $\alpha_{k,n}$ at some constants, problem (7) would still be nonconvex in $\mathbf{w}_{k,n}$. It is not straightforward to even find a feasible solution that satisfies constraints (6b)-(6d).

In principle, both problems (6) and (7) could be solved by the d.c. optimization framework of [29] and [30], where each function $f_{k,n}(\mathbf{w},\alpha_{k,n})$ in the objective (6a) would be recast as a d.c. (difference of two convex functions) function in numerous constrained additional variables. The objective $\min_{k\in\mathcal{K},n\in\mathcal{N}_k} f_{k,n}(\mathbf{w},\alpha_{k,n})$ in (6a) would then be represented as a difference of a convex nonsmooth function and a smooth convex function for the d.c. iteration technique of [31] to apply. In this paper, we will develop a new and more efficient approach to solve problem (7).

As observed in [32], for $\bar{\mathbf{w}}_{k,n} = e^{-\jmath\cdot\arg(\mathbf{h}^H_{k,k,n}\mathbf{w}_{k,n})}\mathbf{w}_{k,n}$, one has $|\mathbf{h}^H_{k,k,n}\mathbf{w}_{k,n}| = \mathbf{h}^H_{k,k,n}\bar{\mathbf{w}}_{k,n} = \Re\{\mathbf{h}^H_{k,k,n}\bar{\mathbf{w}}_{k,n}\} \ge 0$ and $|\mathbf{h}^H_{k',k,n'}\mathbf{w}_{k,n}| = |\mathbf{h}^H_{k',k,n'}\bar{\mathbf{w}}_{k,n}|$ for $(k',n') \ne (k,n)$ and $\jmath \triangleq \sqrt{-1}$. The original problem (7) is thus equivalent to the

[1] The value of $\zeta_{k,n}$ is typically in the range of $0.4-0.6$ for practical energy harvesting circuits [5].

following optimization problem:

$$\max_{\substack{\mathbf{w}_{k,n}\in\mathbb{C}^{M\times 1},\\ \alpha_{k,n}\in(0,1),\\ \forall\ k\in\mathcal{K},\ n\in\mathcal{N}_k}} \ \min_{k\in\mathcal{K},n\in\mathcal{N}_k} f_{k,n}(\mathbf{w},\alpha_{k,n}) \triangleq \frac{(\Re\{\mathbf{h}_{k,k,n}^H\mathbf{w}_{k,n}\})^2}{\varphi_{k,n}(\mathbf{w},\alpha_{k,n})} \quad (8a)$$

$$\text{s.t.}\Re\{\mathbf{h}_{k,k,n}^H\mathbf{w}_{k,n}\}\geq 0,\ \forall\ k\in\mathcal{K},\ n\in\mathcal{N}_k, \quad (8b)$$

$$(6b),(6c),(6d) \quad (8c)$$

Since the function $\tilde{f}_{k,n}(\mathbf{w}_{k,n},t)\triangleq(\Re\{\mathbf{h}_{k,k,n}^H\mathbf{w}_{k,n}\})^2/t$ is convex in $\mathbf{w}_{k,n}\in\mathbb{C}^{M\times 1}$ and $t>0$ [26], it is true that [33]

$$\begin{aligned}\tilde{f}_{k,n}(\mathbf{w}_{k,n},t)&\geq \tilde{f}_{k,n}(\mathbf{w}_{k,n}^{(\kappa)},t^{(\kappa)})\\ &\quad+\langle\nabla\tilde{f}_{k,n}(\mathbf{w}_{k,n}^{(\kappa)},t^{(\kappa)}),(\mathbf{w}_{k,n},t)-(\mathbf{w}_{k,n}^{(\kappa)},t^{(\kappa)})\rangle\\ &=2\Re\left\{\mathbf{h}_{k,k,n}^H\mathbf{w}_{k,n}^{(\kappa)}\right\}\Re\left\{\mathbf{h}_{k,k,n}^H\mathbf{w}_{k,n}\right\}/t^{(\kappa)}\\ &\quad-\left(\Re\left\{\mathbf{h}_{k,k,n}^H\mathbf{w}_{k,n}^{(\kappa)}\right\}\right)^2 t/(t^{(\kappa)})^2 \end{aligned} \quad (9)$$

for all $\mathbf{w}_{k,n}\in\mathbb{C}^{M\times 1},\mathbf{w}_{k,n}^{(\kappa)}\in\mathbb{C}^{M\times 1},t>0,t^{(\kappa)}>0$. Therefore, given $(\mathbf{w}^{(\kappa)},\alpha^{(\kappa)})$ from $\kappa$-th iteration, substituting $t:=\varphi_{k,n}(\mathbf{w},\alpha_{k,n})$ and $t^{(\kappa)}:=\varphi_{k,n}(\mathbf{w}^{(\kappa)},\alpha_{k,n}^{(\kappa)})$ into the above inequality (9) gives

$$f_{k,n}(\mathbf{w},\alpha_{k,n})\geq f_{k,n}^{(\kappa)}(\mathbf{w},\alpha_{k,n}),\ \forall(\mathbf{w},\alpha_{k,n}) \quad (10)$$

where

$$\begin{aligned}f_{k,n}^{(\kappa)}(\mathbf{w},\alpha_{k,n})\triangleq&\frac{2\Re\left\{(\mathbf{w}_{k,n}^{(\kappa)})^H\mathbf{h}_{k,k,n}\right\}\Re\left\{\mathbf{h}_{k,k,n}^H\mathbf{w}_{k,n}\right\}}{\varphi_{k,n}(\mathbf{w}^{(\kappa)},\alpha_{k,n}^{(\kappa)})}\\ &-\frac{\left(\Re\left\{\mathbf{h}_{k,k,n}^H\mathbf{w}_{k,n}^{(\kappa)}\right\}\right)^2\varphi_{k,n}(\mathbf{w},\alpha_{k,n})}{\varphi_{k,n}^2(\mathbf{w}^{(\kappa)},\alpha_{k,n}^{(\kappa)})}\end{aligned} \quad (11)$$

The function $f_{k,n}^{(\kappa)}(\mathbf{w},\alpha_{k,n})$ is concave quadratic and agrees with $f_{k,n}(\mathbf{w},\alpha_{k,n})$ at $(\mathbf{w}^{(\kappa)},\alpha_{k,n}^{(\kappa)})$ as:

$$f_{k,n}(\mathbf{w}^{(\kappa)},\alpha_{k,n}^{(\kappa)})=f_{k,n}^{(\kappa)}(\mathbf{w}^{(\kappa)},\alpha_{k,n}^{(\kappa)}). \quad (12)$$

Next, the nonconvex energy harvesting constraint (6d) can be expressed as

$$\frac{e_{k,n}^{\min}}{\zeta_{k,n}(1-\alpha_{k,n})}-p_{k,n}(\mathbf{w})\leq 0,\ \forall k\in\mathcal{K},n\in\mathcal{N}_k, \quad (13)$$

which is still nonconvex. From

$$\begin{aligned}|\mathbf{h}_{\bar{k},k,n}^H\mathbf{w}_{\bar{k},\bar{n}}|^2\geq&-|\mathbf{h}_{\bar{k},k,n}^H\mathbf{w}_{\bar{k},\bar{n}}^{(\kappa)}|^2\\ &+2\Re\left\{\left(\mathbf{w}_{\bar{k},\bar{n}}^{(\kappa)}\right)^H\mathbf{h}_{\bar{k},k,n}\mathbf{h}_{\bar{k},k,n}^H\mathbf{w}_{\bar{k},\bar{n}}\right\},\\ &\forall\mathbf{w}_{\bar{k},\bar{n}},\mathbf{w}_{\bar{k},\bar{n}}^{(\kappa)}\end{aligned} \quad (14)$$

it follows that

$$p_{k,n}(\mathbf{w})\geq p_{k,n}^{(\kappa)}(\mathbf{w}),\ \forall\mathbf{w}\quad\text{and}\quad p_{k,n}(\mathbf{w}^{(\kappa)})=p_{k,n}^{(\kappa)}(\mathbf{w}^{(\kappa)}) \quad (15)$$

where

$$\begin{aligned}p_{k,n}^{(\kappa)}(\mathbf{w})\triangleq&-p_{k,n}(\mathbf{w}^{(\kappa)})\\ &+2\sum_{\bar{k}\in\mathcal{K}}\sum_{\bar{n}\in\mathcal{N}_{\bar{k}}}\Re\left\{(\mathbf{w}_{\bar{k},\bar{n}}^{(\kappa)})^H\mathbf{h}_{\bar{k},k,n}\mathbf{h}_{\bar{k},k,n}^H\mathbf{w}_{\bar{k},\bar{n}}\right\}.\end{aligned}$$

**Algorithm 1** QP-based Iterative Optimization to Solve Problem (7)

1: Initialize $\kappa:=0$.
2: Choose a feasible point $(\mathbf{w}_{k,n}^{(0)},\alpha_{k,n}^{(0)}),\ \forall k\in\mathcal{K},n\in\mathcal{N}_k$ of (7).
3: **repeat**
4: Solve QP (17) for $\mathbf{w}_{k,n}^{(\kappa+1)}$ and $\alpha_{k,n}^{(\kappa+1)},\ \forall k\in\mathcal{K},n\in\mathcal{N}_k$.
5: Set $\kappa:=\kappa+1$.
6: **until** convergence of the objective in (7).

Therefore, whenever $(\mathbf{w}^{(\kappa)},\alpha^{(\kappa)})$ is feasible to (6d), the nonconvex constraint (6d) is inner-approximated by the convex constraint

$$\frac{e_{k,n}^{\min}}{\zeta_{k,n}(1-\alpha_{k,n})}-p_{k,n}^{(\kappa)}(\mathbf{w})\leq\sigma_a^2,\ \forall k\in\mathcal{K},n\in\mathcal{N}_k. \quad (16)$$

From (12) and (16), for a given $(\mathbf{w}_{k,n}^{(\kappa)},\alpha_{k,n}^{(\kappa)})$ the following convex quadratic program (QP) provides minorant maximization for the nonconvex program (7):

$$\begin{aligned}\max_{\substack{\mathbf{w}_{k,n}\in\mathbb{C}^{M\times 1},\\ \alpha_{k,n}\in(0,1),\\ \forall k\in\mathcal{K},n\in\mathcal{N}_k}}\ &\min_{\substack{k\in\mathcal{K}\\ n\in\mathcal{N}_k}} f_{k,n}^{(\kappa)}(\mathbf{w},\alpha_{k,n})\\ &\text{s.t.}\quad(6b),(6c),(8b),(16).\end{aligned} \quad (17)$$

Using (17), we propose in Algorithm 1 a QP-based iterative algorithm that solves the max-min SINR problem (7). Here, the initial point $\mathbf{w}^{(0)}\triangleq[\mathbf{w}_{k,n}^{(0)}]_{k\in\mathcal{K},n\in\mathcal{N}_k}$ can be found by randomly generating $M\times 1$ complex vectors followed by normalizing them to satisfy (6b) and (6c). For a given $\mathbf{w}^{(0)}$, $\boldsymbol{\alpha}^{(0)}\triangleq[\alpha_{k,n}^{(0)}]_{k\in\mathcal{K},n\in\mathcal{N}_k}$ is then generated by solving (6d) with an equality sign. In each iteration of Algorithm 1, only one simple QP (17) needs to be solved. The solution of which is then used to improve the objective value in the next iteration.

*Proposition 1:* Algorithm 1 generates a sequence $\{(\mathbf{w}^{(\kappa)},\boldsymbol{\alpha}^{(\kappa)})\}$ of improved points for (7), which converges to a Karush-Kuhn-Tucker (KKT) point.

*Proof:* Let us define

$$\begin{aligned}F(\mathbf{w},\boldsymbol{\alpha})&\triangleq\min_{\substack{k\in\mathcal{K}\\ n\in\mathcal{N}_k}} f_{k,n}(\mathbf{w},\alpha_{k,n})\quad\text{and}\\ F^{(\kappa)}(\mathbf{w},\boldsymbol{\alpha})&\triangleq\min_{\substack{k\in\mathcal{K}\\ n\in\mathcal{N}_k}} f_{k,n}^{(\kappa)}(\mathbf{w},\alpha_{k,n}),\end{aligned}$$

which satisfies [cf. (10) and (12)]

$$\begin{aligned}F^{(\kappa)}(\mathbf{w},\boldsymbol{\alpha})&\geq F^{(\kappa)}(\mathbf{w},\boldsymbol{\alpha})\ \forall\ \mathbf{w},\boldsymbol{\alpha}\quad\text{and}\\ F^{(\kappa)}(\mathbf{w}^{(\kappa)},\boldsymbol{\alpha}^{(\kappa)})&=F^{(\kappa)}(\mathbf{w}^{(\kappa)},\boldsymbol{\alpha}^{(\kappa)}).\end{aligned}$$

Hence,

$$\begin{aligned}F(\mathbf{w}^{(\kappa+1)},\boldsymbol{\alpha}^{(\kappa+1)})&\geq F^{(\kappa)}(\mathbf{w}^{(\kappa+1)},\boldsymbol{\alpha}^{(\kappa+1)})\\ &>F^{(\kappa)}(\mathbf{w}^{(\kappa)},\boldsymbol{\alpha}^{(\kappa)})=F(\mathbf{w}^{(\kappa)},\boldsymbol{\alpha}^{(\kappa)}),\end{aligned}$$

where the second inequality follows from the fact that $(\mathbf{w}^{(\kappa+1)},\boldsymbol{\alpha}^{(\kappa+1)})$ and $(\mathbf{w}^{(\kappa)},\boldsymbol{\alpha}^{(\kappa)})$ are the optimal solution

and a feasible point of (17), respectively. This result shows that $(\mathbf{w}^{(\kappa+1)}, \boldsymbol{\alpha}^{(\kappa+1)})$ is a better point to (7) than $(\mathbf{w}^{(\kappa)}, \boldsymbol{\alpha}^{(\kappa)})$.

Furthermore, the sequence $\{(\mathbf{w}^{(\kappa)}, \boldsymbol{\alpha}^{(\kappa)})\}$ is bounded by constraints (6b) and (6c). By Cauchy's theorem, there is a convergent subsequence $\{(\mathbf{w}^{(\kappa_\nu)}, \boldsymbol{\alpha}^{(\kappa_\nu)})\}$ with a limit point $(\bar{\mathbf{w}}, \bar{\alpha})$, i.e.,

$$\lim_{\nu\to+\infty}\Big[F(\mathbf{w}^{(\kappa_\nu)}, \boldsymbol{\alpha}^{(\kappa_\nu)}) - F(\bar{\mathbf{w}}, \bar{\alpha})\Big] = 0.$$

For every $\kappa$, there is $\nu$ such that $\kappa_\nu \le \kappa \le \kappa_{\nu+1}$, and so

$$\begin{aligned} 0 &= \lim_{\nu\to+\infty}[F(\mathbf{w}^{(\kappa_\nu)}, \boldsymbol{\alpha}^{(\kappa_\nu)}) - F(\bar{\mathbf{w}}, \bar{\alpha})] \\ &\le \lim_{\kappa\to+\infty}[F(\mathbf{w}^{(\kappa)}, \boldsymbol{\alpha}^{(\kappa)}) - F(\bar{\mathbf{w}}, \bar{\alpha})] \\ &\le \lim_{\nu\to+\infty}[F(\mathbf{w}^{(\kappa_{\nu+1})}, \boldsymbol{\alpha}^{(\kappa_{\nu+1})}) - F(\bar{\mathbf{w}}, \bar{\alpha})] = 0, \end{aligned} \tag{18}$$

which shows that $\lim_{\kappa\to+\infty} F(\mathbf{w}^{(\kappa)}, \boldsymbol{\alpha}^{(\kappa)}) = F(\bar{\mathbf{w}}, \bar{\alpha})$. Each accumulation point $\{(\bar{\mathbf{w}}, \bar{\boldsymbol{\alpha}})\}$ of the sequence $\{(\mathbf{w}^{(\kappa)}, \boldsymbol{\alpha}^{(\kappa)})\}$ is indeed a KKT point according to [34, Th. 1]. ∎

It is noteworthy that our simulation results in Sec. IV further show that the QP-based solution in Algorithm 1 achieves the *upper bound* given by the SDR (A.1) described in Appendix A.

### *B. Iterative Optimization for Min-Max BS Power*

Next, we will address the min-max BS power optimization problem, which targets minimizing the highest BS radiation power. The motivation is to limit an undue interference from any BS to the neighboring cell users. Therefore, the interference (and hence throughput) at individual users is balanced across the whole network. The min-max BS power optimization problem is formulated as follows:

$$\min_{\substack{\mathbf{w}_{k,n}\in\mathbb{C}^{M\times 1},\\ \alpha_{k,n}\in(0,1),\\ \forall\ k\in\mathcal{K},\ n\in\mathcal{N}_k}} \max_{k\in\mathcal{K}} \sum_{n\in\mathcal{N}_k} \|\mathbf{w}_{k,n}\|^2 \quad \text{s.t.} \quad (6d), \tag{19a}$$

$$|\mathbf{h}_{k,k,n}^H \mathbf{w}_{k,n}|^2 \ge \gamma_{k,n}^{\min}\varphi_{k,n}(\mathbf{w}, \alpha_{k,n}), \quad \forall k\in\mathcal{K}, n\in\mathcal{N}_k. \tag{19b}$$

Here, (6d) requires that the amount of energy harvested by UE $(k,n)$ exceeds some target $e_{k,n}^{\min}$ for useful EH, whereas (19b) ensures a minimum throughput $\ln\left(1+\gamma_{k,n}^{\min}\right)$ for each UE $(k,n)$. Similar to the max-min SINR problem (7), this problem (19) is nonconvex due to the strong coupling between $\mathbf{w}_{k,n}$ and $\alpha_{k,n}$ in the harvested energy expression (5).

Given that the SINR constraint (19b) can be expressed as a second-order cone (SOC) constraint[2], we now address problem (19) via second-order cone programming (SOCP) in the vector variables $\mathbf{w}_{k,n} \in \mathbb{C}^{M\times 1}$. Similar to (8b), we make the variable change $\alpha_{k,n} \to \alpha_{k,n}^2$ in (19) to express (19b) as:

$$\Re\left\{\mathbf{h}_{k,k,n}^H \mathbf{w}_{k,n}\right\} \ge \sqrt{\gamma_{k,n}^{\min}}\sqrt{\varphi_{k,n}(\mathbf{w}, \alpha_{k,n}^2)},\ \forall k\in\mathcal{K}, n\in\mathcal{N}_k, \tag{20}$$

[2]This only means the SINR function is quasi-convex. Therefore, the SOCP-based optimization approach cannot be applied to solve problem (7).

**Algorithm 2** SOC-based Iterative Optimization to Solve Problem (19)

1: Initialize $\kappa := 0$.
2: Choose a feasible point $(\mathbf{w}_{k,n}^{(0)}, \alpha_{k,n}^{(0)}),\ \forall k\in\mathcal{K}, n\in\mathcal{N}_k$ of (19).
3: **repeat**
4: Solve SOCP (24) for $\mathbf{w}_{k,n}^{(\kappa+1)}$ and $\alpha_{k,n}^{(\kappa+1)},\ \forall k\in\mathcal{K}, n\in\mathcal{N}_k$.
5: Set $\kappa := \kappa + 1$.
6: **until** convergence of the objective (19).

which is equivalent to the following SOC:

$$\Re\{\mathbf{h}_{k,k,n}^H \mathbf{w}_{k,n}\} \ge \sqrt{\gamma_{k,n}^{\min}}\left\|\begin{matrix}\sigma_a\\ \sigma_c t_{k,n}\\ \left(\mathbf{h}_{\bar{k},k,n}^H \mathbf{w}_{\bar{k},\bar{n}}\right)_{\bar{k},\bar{n}\in\mathcal{K},\mathcal{N}\setminus\{k,n\}}\end{matrix}\right\|_2, \quad \forall k\in\mathcal{K}, n\in\mathcal{N}, \tag{21}$$

$$\begin{pmatrix} t_{k,n} & 1\\ 1 & \alpha_{k,n}\end{pmatrix} \succeq 0,\ \forall\ k\in\mathcal{K}, n\in\mathcal{N}, \tag{22}$$

where $\left(\mathbf{h}_{\bar{k},k,n}^H \mathbf{w}_{\bar{k},\bar{n}}\right)_{\bar{k},\bar{n}\in\mathcal{K},\mathcal{N}\setminus\{k,n\}}$ is an $(KN-1)\times 1$ column vector. On the other hand, under the variable change $\alpha_{k,n} \to \alpha_{k,n}^2$ in (16), the harvested energy expression (5) is inner-approximated by the following convex constraints:

$$\frac{e_{k,n}^{\min}}{\zeta_{k,n}(1-\alpha_{k,n}^2)} - p_{k,n}^{(\kappa)}(\mathbf{w}) \le \sigma_a^2,\ \forall k\in\mathcal{K}, n\in\mathcal{N}_k. \tag{23}$$

As $(\mathbf{w}^{(\kappa)}, \alpha^{(\kappa)})$ is also feasible to (23), the optimal solution $(\mathbf{w}^{(\kappa+1)}, \alpha^{(\kappa+1)})$ of the following convex program is a better point to (19) than $(\mathbf{w}^{(\kappa)}, \alpha^{(\kappa)})$

$$\min_{\substack{\mathbf{w}_{k,n}\in\mathbb{C}^{M\times 1}\\ \alpha_{k,n}\in(0,1),\ t_{k,n}\\ \forall k\in\mathcal{K}, n\in\mathcal{N}_k}} \max_{k\in\mathcal{K}} \sum_{n\in\mathcal{N}_k} \|\mathbf{w}_{k,n}\|^2 \quad \text{s.t.} \quad (21), (22), (23). \tag{24}$$

In Algorithm 2, we propose an SOC-based iterative algorithm to solve problem (19). In order to obtain an initial feasible point to SOCP (24), we cannot use the inner-approximated EH constraint (23) due to its dependence on the previously optimized beamforming vector $\mathbf{w}^{(\kappa)}$. However, the original EH constraint (6d) can be implied by the following hard (tighter) constraint in $\alpha_{k,n_1}^2$ and a slack variable $\beta_{k,n_1}^2$:

$$\frac{\sqrt{e_{k,n}^{\min}/\zeta_{k,n}}}{\beta_{k,n}} - \Re\{\mathbf{h}_{k,k,n}^H \mathbf{w}_{k,n}\} \le 0, \forall k\in\mathcal{K}, n_1\in\mathcal{N}_k \tag{25a}$$

$$\beta_{k,n}^2 + \alpha_{k,n}^2 \le 1, \forall k\in\mathcal{K}, n\in\mathcal{N}_k, \tag{25b}$$

which is independent of $\mathbf{w}^{(\kappa)}$.[3] Hence, the initial point to SOCP (24) can easily be obtained by solving the following

[3]The satisfaction of the constraint (25) implies the satisfaction of the original EH constraint (6d).

SOCP:

$$\min_{\substack{\mathbf{w}_{k,n}\in\mathbb{C}^{M\times 1},\\ \alpha_{k,n}\in(0,1),\ \beta_{k,n},\ t_{k,n},\\ \forall k\in\mathcal{K},n\in\mathcal{N}_k}} \quad \max_{k\in\mathcal{K}} \quad \sum_{n\in\mathcal{N}_k}\|\mathbf{w}_{k,n}\|^2$$
$$\text{s.t.} \quad (21),(22),(25a),(25b). \tag{26}$$

Once initialized from a feasible point, Algorithm 2 solves one simple convex SOCP (24) in each iteration. The solution of which is then used in the next iteration to improve the objective value. Similar to Proposition 1, it can be shown that Algorithm 2 generates a sequence $\{(\mathbf{w}^{(\kappa)},\boldsymbol{\alpha}^{(\kappa)})\}$ of improved points for problem (19), which converges to a KKT point. Our simulation results in Sec. IV further show that the SOC-based solution in Algorithm 2 achieves the *lower bound* given by the SDR (A.2a), (A.2b), (A.1e), (A.1f) described in Appendix A.

## III. Max-Min Rate and Min-Max Power Optimization for Transmit Time-Switching WIPT Systems

Unlike the power-switching system model in Sec. II, in the time-switching (TS) based system, a fraction of time $0<\rho<1$ is used for power transfer while the remaining fraction of time $(1-\rho)$ for information transfer. Here $\rho$ is termed as the TS ratio. For power transfer, we are to design beamforming vectors $\mathbf{w}_{k,n}^E$ with the achievable harvested energy $\rho E_{k,n}(\mathbf{w}^E)$, where

$$E_{k,n}(\mathbf{w}^E)\triangleq\zeta_{k,n}(p_{k,n}(\mathbf{w}^E)+\sigma_a^2),$$
$$p_{k,n}(\mathbf{w}^E)\triangleq\sum_{\bar{k}\in\mathcal{K}}\sum_{\bar{n}\in\mathcal{N}_{\bar{k}}}|\mathbf{h}_{\bar{k},k,n}^H\mathbf{w}_{\bar{k},\bar{n}}^E|^2,$$

and $\mathbf{w}^E\triangleq[\mathbf{w}_{k,n}^E]_{k\in\mathcal{K},n\in\mathcal{N}_k}$. For information transfer, we are to design beamforming vectors $\mathbf{w}_{k,n}^I$ with the achievable data rate

$$(1-\rho)\ln\left(1+\frac{|\mathbf{h}_{k,k,n}^H\mathbf{w}_{k,n}^I|^2}{\varphi_{k,n}(\mathbf{w}^I)}\right)$$

where

$$\varphi_{k,n}(\mathbf{w}^I)\triangleq\underbrace{\sum_{\bar{n}\in\mathcal{N}_k\setminus\{n\}}|\mathbf{h}_{k,k,n}^H\mathbf{w}_{k,\bar{n}}^I|^2}_{\text{intracell interference}}+\underbrace{\sum_{\bar{k}\in\mathcal{K}\setminus\{k\}}\sum_{\bar{n}\in\mathcal{N}_{\bar{k}}}|\mathbf{h}_{\bar{k},k,n}^H\mathbf{w}_{\bar{k},\bar{n}}^I|^2}_{\text{intercell interference}}+\sigma_a^2,$$

and $\mathbf{w}^I\triangleq[\mathbf{w}_{k,n}^I]_{k\in\mathcal{K},n\in\mathcal{N}_k}$. Therefore, the individual BS and total power constraints for the TS-based system are:

$$\rho\sum_{n\in\mathcal{N}_k}\|\mathbf{w}_{k,n}^E\|^2+(1-\rho)\sum_{n\in\mathcal{N}_k}\|\mathbf{w}_{k,n}^I\|^2\le P_k^{\max},\forall k\in\mathcal{K} \tag{27a}$$

$$\rho\sum_{k\in\mathcal{K}}\sum_{n\in\mathcal{N}_k}\|\mathbf{w}_{k,n}^E\|^2+(1-\rho)\sum_{k\in\mathcal{K}}\sum_{n\in\mathcal{N}_k}\|\mathbf{w}_{k,n}^I\|^2\le P^{\max}, \tag{27b}$$

respectively. Here, the following constraints must also be imposed:

$$\|\mathbf{w}_{k,n}^E\|^2\le P^{\max},\quad \|\mathbf{w}_{k,n}^I\|^2\le P_k^{\max},\ \forall k\in\mathcal{K},n\in\mathcal{N}_k. \tag{28}$$

The max-min rate optimization problem for the TS-based system is then formulated as:

$$\max_{\substack{0<\rho<1,\\ \mathbf{w}_{k,n}^x\in\mathbb{C}^{M\times 1},\,x\in\{I,E\}}}\ \min_{k\in\mathcal{K},n\in\mathcal{N}_k}(1-\rho)\ln(1+f_{k,n}(\mathbf{w}^I)) \tag{29a}$$
$$\text{s.t.}\quad \rho E_{k,n}(\mathbf{w}^E)\ge e_{k,n}^{\min}, \tag{29b}$$
$$(27),(28). \tag{29c}$$

And the min-max BS power optimization problem for the TS-based system is formulated as:

$$\min_{\substack{0<\rho<1,\\ \mathbf{w}_{k,n}^x\in\mathbb{C}^{M\times 1},\,x\in\{E,I\}}}\ \max_{k\in\mathcal{K}}\rho\sum_{n\in\mathcal{N}_k}\|\mathbf{w}_{k,n}^E\|^2+(1-\rho)\sum_{n\in\mathcal{N}_k}\|\mathbf{w}_{k,n}^I\|^2 \tag{30a}$$
$$\text{s.t.}\quad (1-\rho)\ln\left(1+f_{k,n}(\mathbf{w}^I)\right)\ge r_{k,n}^{\min}, \tag{30b}$$
$$(28),(29b) \tag{30c}$$

where (30b) ensures the minimum rate $r_{k,n}^{\min}$ (in nat/sec/Hz) is achieved.

*Remark 1:* The *transmit* TS-based WIPT system is different from the *receive* TS-based WIPT system [10] which switches the received signal $y_{k,n}$ in (1) in the proportion of time $0<\alpha_{k,n}<1$ for information decoding. Accordingly, the joint design of transmit beamformer $\mathbf{w}$ and *receive* TS ratios $\boldsymbol{\alpha}\triangleq[\alpha_{k,n}]_{k\in\mathcal{K},n\in\mathcal{N}_k}$ is formulated as:

$$\max_{\substack{0<\alpha_{k,n}<1,\\ \mathbf{w}_{k,n}\in\mathbb{C}^{M\times 1}}}\ \min_{k\in\mathcal{K},n\in\mathcal{N}_k}(1-\alpha_{k,n})\ln(1+f_{k,n}(\mathbf{w}))$$
$$\text{s.t.}\quad (6b),(6c),\ \text{and}\ \alpha_{k,n}E_{k,n}(\mathbf{w})\ge e_{k,n}^{\min}, \tag{31}$$

and

$$\min_{\substack{0<\alpha_{k,n}<1,\\ \mathbf{w}_{k,n}\in\mathbb{C}^{M\times 1}}}\ \max_{k\in\mathcal{K}}\sum_{n\in\mathcal{N}_k}\|\mathbf{w}_{k,n}\|^2$$
$$\text{s.t.}\quad \alpha_{k,n}E_{k,n}(\mathbf{w})\ge e_{k,n}^{\min},$$
$$(1-\alpha_{k,n})\ln(1+f_{k,n}(\mathbf{w}))\ge r_{k,n}^{\min}. \tag{32}$$

Compared with the receive PS-based optimization problems (7) and (19), the power and EH constraints in (31) and (32) remain the same while the data rate in (31) and (32) is lower. The receive PS-based design thus outperforms the *receive* TS-based design in general. On the other hand, the *transmit* TS-based optimizations (29) and (30) exploit the separate designs of $\mathbf{w}^I$ for ID and $\mathbf{w}^E$ for EH. For this reason, they outperform the receive PS-based designs in (7) and (19) as will be shown later.

### A. Iterative Max-Min Rate Optimization

We will now solve the nonconvex problem (29). First, let us make the following change of variable:

$$1-\rho=1/\beta, \tag{33}$$

which satisfies the linear constraint

$$\beta>1. \tag{34}$$

Thus, the power constraints (27) become the following convex constraints:

$$\sum_{n\in\mathcal{N}_k}\|\mathbf{w}_{k,n}^E\|^2+\frac{1}{\beta}\sum_{n\in\mathcal{N}_k}\|\mathbf{w}_{k,n}^I\|^2\le P_k^{\max}+\frac{1}{\beta}\sum_{n\in\mathcal{N}_k}\|\mathbf{w}_{k,n}^E\|^2,\ \forall k\in\mathcal{K} \tag{35a}$$

$$\sum_{k\in\mathcal{K}}\sum_{n\in\mathcal{N}_k}\|\mathbf{w}_{k,n}^E\|^2+\frac{1}{\beta}\sum_{k\in\mathcal{K}}\sum_{n\in\mathcal{N}_k}\|\mathbf{w}_{k,n}^I\|^2\le P^{\max}+\frac{1}{\beta}\sum_{k\in\mathcal{K}}\sum_{n\in\mathcal{N}_k}\|\mathbf{w}_{k,n}^E\|^2. \tag{35b}$$

Similar to (8), problem (29) can now be equivalently expressed by

$$\max_{\substack{\alpha,\beta,\\ \mathbf{w}_{k,n}^x\in\mathbb{C}^{M\times 1},x\in\{I,E\}}}\ \min_{k\in\mathcal{K},n\in\mathcal{N}_k}\frac{1}{\beta}\ln\left(1+\frac{(\Re\{\mathbf{h}_{k,k,n}^H\mathbf{w}_{k,n}^I\})^2}{\varphi_{k,n}(\mathbf{w}^I)}\right) \tag{36a}$$

$$\text{s.t.}\quad \Re\left\{\mathbf{h}_{k,k,n}^H\mathbf{w}_{k,n}^I\right\}\ge 0,\ \forall k\in\mathcal{K},n\in\mathcal{N}_k, \tag{36b}$$

$$p_{k,n}(\mathbf{w}^E)\ge\frac{e_{k,n}^{\min}}{\zeta_{k,n}}\left(1+\frac{1}{\beta-1}\right)-\sigma_a^2, \tag{36c}$$

$$(28),(34),(35). \tag{36d}$$

Note that unlike (8), the objective function in (36) is quite complex to handle due to the additional factor $1/\beta$, while the power constraint (35) is nonconvex. To deal with this, we first exploit the fact that function $f(x,t)=\frac{\ln(1+1/x)}{t}$ is convex in $x>0,t>0$ which can be seen by examining its Hessian. The following inequality for all $x>0$, $\bar{x}>0$, $t>0$ and $\bar{t}>0$ then holds true:

$$\begin{aligned}\frac{\ln(1+1/x)}{t}&\ge f(\bar{x},\bar{t})+\langle\nabla f(\bar{x},\bar{t}),(x,t)-(\bar{x},\bar{t})\rangle\\&=2\frac{\ln(1+1/\bar{x})}{\bar{t}}+\frac{1}{\bar{t}(\bar{x}+1)}-\frac{x}{(\bar{x}+1)\bar{x}\bar{t}}\\&\quad-\frac{\ln(1+1/\bar{x})}{\bar{t}^2}t.\end{aligned} \tag{37}$$

By replacing $1/x\to x$ and $1/\bar{x}\to\bar{x}$ in (37), we have:

$$\frac{\ln(1+x)}{t}\ge a-\frac{b}{x}-ct, \tag{38}$$

where $a=2\frac{\ln(1+\bar{x})}{\bar{t}}+\frac{\bar{x}}{\bar{t}(\bar{x}+1)}>0, b=\frac{\bar{x}^2}{\bar{t}(\bar{x}+1)}>0, c=\frac{\ln(1+\bar{x})}{\bar{t}^2}>0$. From that,

$$\frac{1}{\beta}\ln\left(1+\frac{\left(\Re\{\mathbf{h}_{k,k,n}^H\mathbf{w}_{k,n}^I\}\right)^2}{\varphi_{k,n}(\mathbf{w}^I)}\right)\ge a^{(\kappa)}-b^{(\kappa)}\frac{\varphi_{k,n}(\mathbf{w}^I)}{\left(\Re\left\{\mathbf{h}_{k,k,n}^H\mathbf{w}_{k,n}^I\right\}\right)^2}-c^{(\kappa)}\beta \tag{39}$$

where

$$\begin{aligned}a^{(\kappa)}&=2\frac{\ln(1+d^{(\kappa)})}{\beta^{(\kappa)}}+\frac{d^{(\kappa)}}{\beta^{(\kappa)}(d^{(\kappa)}+1)}>0,\\b^{(\kappa)}&=\frac{(d^{(\kappa)})^2}{\beta^{(\kappa)}(d^{(\kappa)}+1)}>0,\\c^{(\kappa)}&=\frac{\ln(1+d^{(\kappa)})}{(\beta^{(\kappa)})^2}>0,\\d^{(\kappa)}&=\left(\Re\left\{\mathbf{h}_{k,k,n}^H\mathbf{w}_{k,n}^{I,(\kappa)}\right\}\right)^2/\varphi_{k,n}(\mathbf{w}^{I,(\kappa)}).\end{aligned} \tag{40}$$

Now, using

$$\begin{aligned}\left(\Re\left\{\mathbf{h}_{k,k,n}^H\mathbf{w}_{k,n}^I\right\}\right)^2&\ge 2\Re\{\mathbf{h}_{k,k,n}^H\mathbf{w}_{k,n}^{I,(\kappa)}\}\Re\left\{\mathbf{h}_{k,k,n}^H\mathbf{w}_{k,n}^I\right\}\\&\quad-\left(\Re\left\{\mathbf{h}_{k,k,n}^H\mathbf{w}_{k,n}^{I,(\kappa)}\right\}\right)^2\\&\triangleq\psi_{k,n}(\mathbf{w}_{k,n}^I)\end{aligned}$$

together with (39) leads to

$$\begin{aligned}\frac{1}{\beta}\ln\left(1+\frac{\left(\Re\left\{\mathbf{h}_{k,k,n}^H\mathbf{w}_{k,n}^I\right\}\right)^2}{\varphi_{k,n}(\mathbf{w}^I)}\right)&\ge a^{(\kappa)}-b^{(\kappa)}\frac{\varphi_{k,n}(\mathbf{w}^I)}{\psi_{k,n}(\mathbf{w}_{k,n}^I)}\\&\quad-c^{(\kappa)}\beta\\&\triangleq f_{k,n}^{(\kappa)}(\mathbf{w}^I,\beta)\end{aligned} \tag{41}$$

for

$$\psi_{k,n}(\mathbf{w}_{k,n}^I)\ge 0,\ \forall k\in\mathcal{K},n\in\mathcal{N}_k. \tag{42}$$

As the function $f_{k,n}^{(\kappa)}(\mathbf{w}^I,\beta)$ is concave on (42), the following convex program provides minorant maximization for the nonconvex program (36) for a given $(\mathbf{w}^{E,(\kappa)},\mathbf{w}^{I,(\kappa)},\beta^{(\kappa)})$:

$$\max_{\substack{\beta,\\ \mathbf{w}_{k,n}^x\in\mathbb{C}^{M\times 1},\,x\in\{I,E\}}}\ \min_{k\in\mathcal{K},n\in\mathcal{N}_k}f_{k,n}^{(\kappa)}(\mathbf{w}^I,\beta) \tag{43a}$$

$$\begin{aligned}\text{s.t}\quad&\sum_{n\in\mathcal{N}_k}\|\mathbf{w}_{k,n}^E\|^2+\frac{1}{\beta}\sum_{n\in\mathcal{N}_k}\|\mathbf{w}_{k,n}^I\|^2\le P_k^{\max}\\&\quad+\frac{1}{\beta^{(\kappa)}}\sum_{n\in\mathcal{N}_k}2\Re\left\{(\mathbf{w}_{k,n}^{E,(\kappa)})^H\mathbf{w}_{k,n}^E\right\}\\&\quad-\frac{\beta}{(\beta^{(\kappa)})^2}\sum_{n\in\mathcal{N}_k}\|\mathbf{w}_{k,n}^{E,(\kappa)}\|^2,\ \forall k\in\mathcal{K},\end{aligned} \tag{43b}$$

$$\begin{aligned}&\sum_{k\in\mathcal{K}}\sum_{n\in\mathcal{N}_k}\|\mathbf{w}_{k,n}^E\|^2+\frac{1}{\beta}\sum_{k\in\mathcal{K}}\sum_{n\in\mathcal{N}_k}\|\mathbf{w}_{k,n}^I\|^2\le P^{\max}\\&\quad+\frac{1}{\beta^{(\kappa)}}\sum_{k\in\mathcal{K}}\sum_{n\in\mathcal{N}_k}2\Re\left\{(\mathbf{w}_{k,n}^{E,(\kappa)})^H\mathbf{w}_{k,n}^E\right\}\\&\quad-\frac{\beta}{(\beta^{(\kappa)})^2}\sum_{k\in\mathcal{K}}\sum_{n\in\mathcal{N}_k}\|\mathbf{w}_{k,n}^{E,(\kappa)}\|^2,\end{aligned} \tag{43c}$$

$$\begin{aligned}&\sum_{\bar{k}\in\mathcal{K}}\sum_{\bar{n}\in\mathcal{N}_{\bar{k}}}\Big[2\Re\left\{\mathbf{h}_{\bar{k},k,n}^H\mathbf{w}_{\bar{k},\bar{n}}^{E,(\kappa)}\mathbf{h}_{\bar{k},k,n}^H\mathbf{w}_{\bar{k},\bar{n}}^E\right\}\\&\quad-\left|\mathbf{h}_{\bar{k},k,n}^H\mathbf{w}_{\bar{k},\bar{n}}^{E,(\kappa)}\right|^2\Big]\ge\frac{e_{k,n}^{\min}}{\zeta_{k,n}}\left(1+\frac{1}{\beta-1}\right)-\sigma_a^2,\end{aligned} \tag{43d}$$

$$(28),(34),(36b),(42) \tag{43e}$$

**Algorithm 3** Iterative Optimization to Solve Problem (36)

1: Initialize $\kappa := 0$.
2: Choose a feasible point $\left(\mathbf{w}^{E,(0)}, \mathbf{w}^{I,(0)}, \beta^{(0)}\right)$ of (36).
3: **repeat**
4: Solve convex program (43) for $\left(\mathbf{w}^{E,(\kappa+1)}, \mathbf{w}^{I,(\kappa+1)}, \beta^{(\kappa+1)}\right)$.
5: Set $\kappa := \kappa + 1$.
6: **until** convergence of the objective in (36).

Here, convex constraints (43b), (43c) and (43d) are the inner approximations of nonconvex constraints (35) and (36d) due to the convexity of function $\frac{1}{\beta}\|\mathbf{x}\|^2$, which leads to

$$\frac{\|\mathbf{x}\|^2}{\beta} \geq \frac{2\Re\left\{(\mathbf{x}^{(\kappa)})^H\mathbf{x}\right\}}{\beta^{(\kappa)}} - \frac{\|\mathbf{x}^{(\kappa)}\|^2}{(\beta^{(\kappa)})^2}\beta, \quad \forall \mathbf{x} \in \mathbb{C}^N, \mathbf{x}^{(\kappa)} \in \mathbb{C}^N, \beta > 0, \beta^{(\kappa)} > 0. \quad (44)$$

The proposed solution for the max-min rate problem (36) (and hence (29)) is summarized in Algorithm 3. Similar to Proposition 1, it can be shown that Algorithm 3 generates a sequence $\left\{\left(\mathbf{w}^{E,(\kappa)}, \mathbf{w}^{I,(\kappa)}, \beta^{(\kappa)}\right)\right\}$ of improved points of (36), which converges to a KKT point. In Algorithm 3, the feasible point $\left(\mathbf{w}^{E,(0)}, \mathbf{w}^{I,(0)}, \beta^{(0)}\right)$ of (36) is found as follows. We fix $\beta^{(0)}$ and solve the following convex problem for fixed $r_{\min} > 0$:

$$\max_{\mathbf{w}^x_{k,n}\in\mathbb{C}^{M\times 1}, x\in\{I,E\}} \min_{k\in\mathcal{K}, n\in\mathcal{N}_k} \Re\left\{\mathbf{h}^H_{k,k,n}\mathbf{w}^E_{k,n}\right\} - \sqrt{e^{\min}_{k,n}/\left(\zeta_{k,n}\left(1-1/\beta^{(0)}\right)\right)}, \quad (45a)$$

$$\text{s.t.} \quad \Re\left\{\mathbf{h}^H_{k,k,n}\mathbf{w}^I_{k,n}\right\} \geq \sqrt{e^{r^{\min}\beta^{(0)}}-1} \times \left\|\left(\mathbf{h}^H_{\bar{k},k,n}\mathbf{w}^I_{\bar{k},\bar{n}}\right)_{\bar{k},\bar{n}\in\mathcal{K},\mathcal{N}\setminus\{k,n\}}\right\|_2, \quad k \in \mathcal{K}, n \in \mathcal{N}, \quad (45b)$$

$$\left(1-1/\beta^{(0)}\right)\sum_{n\in\mathcal{N}_k}\|\mathbf{w}^E_{k,n}\|^2 + \left(1/\beta^{(0)}\right) \times \sum_{n\in\mathcal{N}_k}\|\mathbf{w}^I_{k,n}\|^2 \leq P^{\max}_k, \ \forall k \in \mathcal{K}, \quad (45c)$$

$$\left(1-1/\beta^{(0)}\right)\sum_{k\in\mathcal{K}}\sum_{n\in\mathcal{N}_k}\|\mathbf{w}^E_{k,n}\|^2 + \left(1/\beta^{(0)}\right) \times \sum_{k\in\mathcal{K}}\sum_{n\in\mathcal{N}_k}\|\mathbf{w}^I_{k,n}\|^2 \leq P^{\max}, \quad (45d)$$

$$(28) \quad (45e)$$

and then iteratively solve the following convex problem:

$$\max_{\mathbf{w}^x_{k,n}\in\mathbb{C}^{M\times 1}, x\in\{I,E\}} \min_{k\in\mathcal{K}, n\in\mathcal{N}_k} \sum_{\bar{k}\in\mathcal{K}}\sum_{\bar{n}\in\mathcal{N}_{\bar{k}}}\left[2\Re\left\{\mathbf{h}^H_{\bar{k},k,n}\mathbf{w}^{E,(\kappa)}_{\bar{k},\bar{n}} \times \mathbf{h}^H_{\bar{k},k,n}\mathbf{w}^E_{\bar{k},\bar{n}}\right\} - \left|\mathbf{h}^H_{\bar{k},k,n}\mathbf{w}^{E,(\kappa)}_{\bar{k},\bar{n}}\right|^2\right] - \frac{e^{\min}_{k,n}}{\zeta_{k,n}}\left(1+\frac{1}{\beta^{(0)}-1}\right) - \sigma_a^2$$

$$\text{s.t.} \quad (28), (45b), (45c), (45d) \quad (46)$$

**Algorithm 4** Iterative Optimization to Solve Problem (47)

1: Initialize $\kappa := 0$.
2: Choose a feasible point $\left(\mathbf{w}^{E,(0)}, \mathbf{w}^{I,(0)}, \beta^{(0)}\right)$ of (47).
3: **repeat**
4: Solve the convex program (48) for $\left(\mathbf{w}^{E,(\kappa+1)}, \mathbf{w}^{I,(\kappa+1)}, \beta^{(\kappa+1)}\right)$.
5: Set $\kappa := \kappa + 1$.
6: **until** convergence of the objective (48).

where the initial point $\mathbf{w}^{E,(0)}_{k,n}$ for (46) is obtained from the solution of (45). Problem (46) is solved for $\kappa = 0, 1, 2, \ldots$ until a positive optimal value is attained. If problem (45) or (46) is infeasible with $\beta^{(0)}$ or solving (46) fails to give a positive optimal value, we repeat the above process for a different value of $\beta^{(0)}$ in order to find a feasible point $\left(\mathbf{w}^{E,(0)}, \mathbf{w}^{I,(0)}, \beta^{(0)}\right)$.[4]

### *B. Iterative Min-Max Power Optimization*

We now turn our attention to the min-max BS power optimization problem (30), which is equivalently expressed as:

$$\min_{\substack{\beta>0,\\ \mathbf{w}^x_{k,n}\in\mathbb{C}^{M\times 1}, x\in\{E,I\}}} \max_{k\in\mathcal{K}} \left[\sum_{n\in\mathcal{N}_k}\|\mathbf{w}^E_{k,n}\|^2 + \frac{1}{\beta}\sum_{n\in\mathcal{N}_k}\|\mathbf{w}^I_{k,n}\|^2 - \frac{1}{\beta}\sum_{n\in\mathcal{N}_k}\|\mathbf{w}^E_{k,n}\|^2\right] \quad (47a)$$

$$\text{s.t.} \quad (28), (34), (36d), \quad (47b)$$

$$\frac{1}{\beta}\ln\left(1+f_{k,n}(\mathbf{w}^I)\right) \geq r^{\min}_{k,n}. \quad (47c)$$

From (41) and (44), the following convex program provides majorant minimization for the nonconvex program (47) for a given $(\mathbf{w}^{E,(\kappa)}_{k,n}, \mathbf{w}^{I,(\kappa)}_{k,n}, \beta^{(\kappa)})$:

$$\min_{\substack{\beta>0,\\ \mathbf{w}^x_{k,n}\in\mathbb{C}^{M\times 1}, x\in\{E,I\}}} \max_{k\in\mathcal{K}} \left[\sum_{n\in\mathcal{N}_k}\|\mathbf{w}^E_{k,n}\|^2 + \frac{1}{\beta}\sum_{n\in\mathcal{N}_k}\|\mathbf{w}^I_{k,n}\|^2 - \frac{1}{\beta^{(\kappa)}}\sum_{n\in\mathcal{N}_k}2\Re\left\{(\mathbf{w}^{E,(\kappa)}_{k,n})^H\mathbf{w}^E_{k,n}\right\} + \frac{\beta}{(\beta^{(\kappa)})^2}\sum_{n\in\mathcal{N}_k}\|\mathbf{w}^{E,(\kappa)}_{k,n}\|^2\right] \quad (48a)$$

$$\text{s.t.} \quad (28), (34), (36b), (42), (43d), \quad (48b)$$

$$f^{(\kappa)}_{k,n}\left(\mathbf{w}^I, \beta\right) \geq r^{\min}_{k,n}, \quad (48c)$$

where $f^{(\kappa)}_{k,n}(\mathbf{w}^I, \beta)$ is defined in (41).

The proposed solution for the min-max BS power optimization problem (47) (and hence (30)) is summarized in Algorithm 4. Similar to Proposition 1, it can be shown that Algorithm 4 generates a sequence $\left\{\left(\mathbf{w}^{E,(\kappa)}, \mathbf{w}^{I,(\kappa)}, \beta^{(\kappa)}\right)\right\}$ of improved points of (48), which converges to a KKT point. In

[4]Simulation results in Sec. IV show that in almost all of the scenarios considered, problems (45) or (46) are feasible and a positive optimal value of (46) is obtained in one single iteration for the first tried value $\beta^{(0)} = 1.11$.

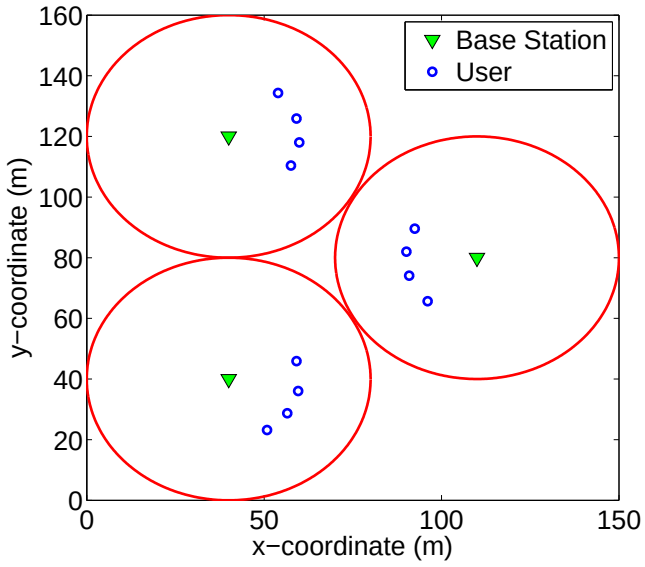


Fig. 2. Topology of the multicell network used in the numerical examples

Algorithm 4, the feasible $\left\{\left(\mathbf{w}^{E,(0)}, \mathbf{w}^{I,(0)}, \beta^{(0)}\right)\right\}$ of (47) can be found by first fixing $\beta^{(0)}$ and solving the convex feasibility problem with the following constraints:

$$\sqrt{e_{k,n}^{\min} / \left(\zeta_{k,n}\left(1 - 1/\beta^{(0)}\right)\right)} - \Re\{\mathbf{h}_{k,k,n}^H \mathbf{w}_{k,n}^E\} \leq 0, \quad k \in \mathcal{K}, n \in \mathcal{N}, \quad (49a)$$

$$\Re\left\{\mathbf{h}_{k,k,n}^H \mathbf{w}_{k,n}^I\right\} \geq \sqrt{e^{r_{k,n}^{\min}\beta^{(0)}} - 1} \times \left\| \left(\mathbf{h}_{\bar{k},k,n}^H \mathbf{w}_{\bar{k},\bar{n}}^I\right)_{\bar{k},\bar{n} \in \mathcal{K}, \mathcal{N}\setminus\{k,n\}}^{\sigma_a} \right\|_2, \quad k \in \mathcal{K}, n \in \mathcal{N}, \quad (49b)$$

(28), (36b). (49c)

## IV. Numerical Examples and Complexity Analysis

In the numerical examples, a 3-cell network model with 4 UEs per cell shown in Fig. 2 is used. The cell radius is set as 40 m and the BS-to-UE distance as 20 m to enable practical WIPT [7], [8]. For large-scale propagation loss, a pathloss exponent equal to 4 is assumed. For small-scale fading, a Rician fading channel is generated according to

$$\mathbf{h}_{\bar{k},k,n} = \sqrt{\frac{K_R}{1+K_R}}\mathbf{h}_{\bar{k},k,n}^{\text{LOS}} + \sqrt{\frac{1}{1+K_R}}\mathbf{h}_{\bar{k},k,n}^{\text{NLOS}}, \ \forall \bar{k}, k, n \quad (50)$$

where $K_R = 10$ dB is the Rician factor; $\mathbf{h}_{\bar{k},k,n}^{\text{LOS}} \in \mathbb{C}_{M\times 1}$ is the line-of-sight (LOS) deterministic component; and $\mathbf{h}_{\bar{k},k,n}^{\text{NLOS}} \sim \mathcal{CN}(0,1)$ is the circularly-symmetric complex Gaussian random variable that models the Rayleigh fading component. Here, the far-field uniform linear antenna array model is used with

$$\mathbf{h}_{\bar{k},k,n}^{\text{LOS}} = \left[1, e^{j\theta_{\bar{k},k,n}}, e^{j2\theta_{\bar{k},k,n}}, \ldots, e^{j(M-1)\theta_{\bar{k},k,n}}\right]^T$$

for $\theta_{\bar{k},k,n} = 2\pi d \sin(\phi_{\bar{k},k,n})/\lambda$, where $d = \lambda/2$ is the antenna spacing, $\lambda$ is the carrier wavelength and $\phi_{\bar{k},k,n}$ is the direction of UE $(k,n)$ to BS $\bar{k}$ [21]. In the simulations, $\phi_{\bar{k},k,n}$ is generated as a random angle between $0^o$ and $360^o$. For simplicity and without loss of generality, we assume that $\gamma_{k,n}^{\min} = \underline{\gamma}$ in (19b), $r_{k,n}^{\min} = \underline{r}$ in (30b), and $\zeta_{k,n} = \zeta$, $e_{k,n}^{\min} = \underline{e}$, $\forall k, n$. Unless specified otherwise, we set the target minimum EH threshold as $\underline{e} = -20$ dBm. In all simulations, we also set $\zeta = 0.5$, $\sigma_a^2 = -90$ dBm and $\sigma_c^2 = -90$ dBm. The error tolerance used in the stopping condition is set as $10^{-3}$ for all algorithms. All simulations are conducted using MATLAB 2015b and CVX 2.1 [35].

### A. Results for Max-Min Rate Problems (7) and (29)

Algorithm 1, the nonsmooth optimization algorithm of [27] and the SDR approach are used to solve the PS-based problem (7), whereas Algorithm 3 is to solve the TS-based problem (29). Assuming that $P^{\max} = 22$ dBW, Figs. 3 and 4 plot the maximized minimum UE rate for different values of BS transmit power $P_k^{\max}$ and BS transmit antenna number $M$. Figs. 3 and 4 show that the minimum UE rate improves by increasing the power budget $P_k^{\max}$ and the number of BS antennas $M$, respectively, due to an increase in the available radio resources. In Fig. 4, we also evaluate the performance of the algorithms for different values of the target minimum EH threshold, $\underline{e} = \{-20, -10\}$ dBm. Fig. 4 shows that by increasing the target EH threshold from $\underline{e} = -20$ dBm to $\underline{e} = -10$ dBm, the achievable information rate is reduced since more time (in the TS-based system) or power (in the PS-based system) is required to meet the increased EH requirement. However, it is important to mention that the percentage of decrease in the information rate for the TS-based system is quite less than that for the PS-based system.

In addition, we can see from Figs. 3 and 4 that the performance of Algorithm 1 coincides with the upper bound obtained by the SDR approach in all the considered simulation setups. Although the proposed algorithm of [27] also achieves

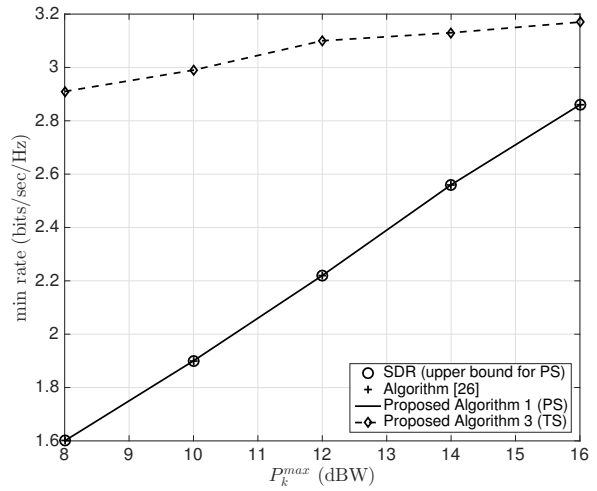


Fig. 3. Maximized minimum UE rate for $M = 4$ and $P^{\max} = 22$ dBW.

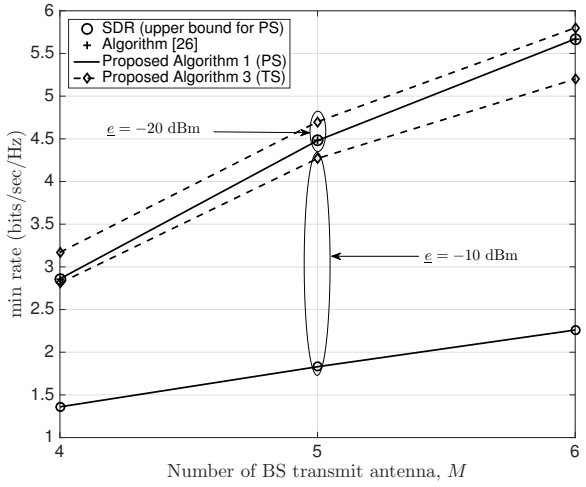


Fig. 4. Maximized minimum UE rate for $P^{\max} = 22$ dBW, $P_k^{\max} = 16$ dBW and $\underline{e} = \{-20, -10\}$ dBm.

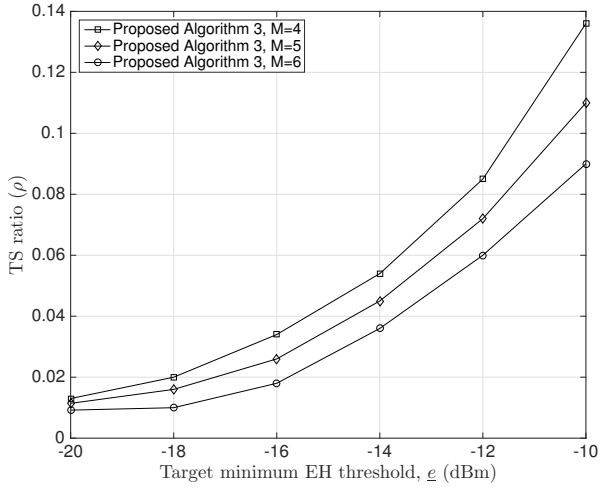


Fig. 5. Optimzed TS ratio $\rho$ by Algorithm 3 for different numbers of BS antennas $M$ and $P_k^{\max} = 16$ dBW.

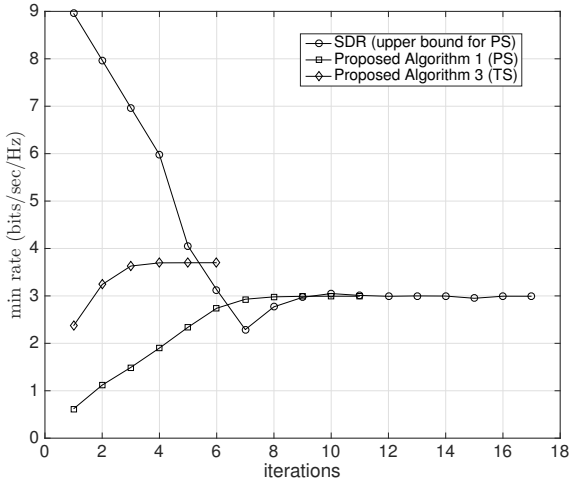


Fig. 6. Convergence of proposed Algorithms 1 and 3 for $M = 4$ and $P_k^{\max} = 16$ dBW.

this bound, it requires much higher computational complexity than Algorithm 1 as will be analyzed shortly. It should be noted that Algorithm 1 does not perform any bisection search as is the case for both the SDR approach and the algorithm of [27]. Note further that the SDR approach only provides rank-one matrices $\mathbf{W}_{k,n}^{\star}$ in no more than $61.7\%$ of the time [27]. In contrast, the nonsmooth optimization algorithm of [27] always returns rank-one matrix solutions, and Algorithm 1 of course directly gives the optimal vectors $\mathbf{w}_{k,n}^{\star}$ because no matrix optimization is involved. Figs. 3 and 4 also show that transmit TS-based WIPT system with Algorithm 3 considerably outperforms the receive PS-based counterpart. Such throughput enhancement is generally not possible with the *receive* TS-based WIPT system as has been reported in the literature. With its high performance and easy implementation, the transmit TS-based solution could be an attractive candidate for practical WIPT systems.

Applying Algorithm 3 for the max-min rate problem (29), Fig. 5 plots the optimized value of the transmit TS ratio $\rho$ for different values of the target EH threshold $\underline{e}$ and the number of BS antennas $M = \{4, 5, 6\}$. As can be seen, by increasing the target EH threshold $\underline{e}$ the optimized TS ratio $\rho$ increases since more time duration is required to fulfill the increased EH requirement. It is further observed that the optimized value of the TS ratio $\rho$ is smaller in the presence of a larger number of BS antennas.

Fig. 6 illustrates the fast convergence of Algorithms 1 and 3 which terminate in as few as $8$ and $4$ iterations, respectively. Here, each iteration corresponds to solving one simple QP (17) in Algorithm 1, one convex problem (43) in Algorithm 3, and one SDP (A.1a)–(A.1f) in the SDR approach. Note that initializing the proposed Algorithms 1 and 3 only requires a single iteration.

The computational complexities of Algorithm 1, the nons-

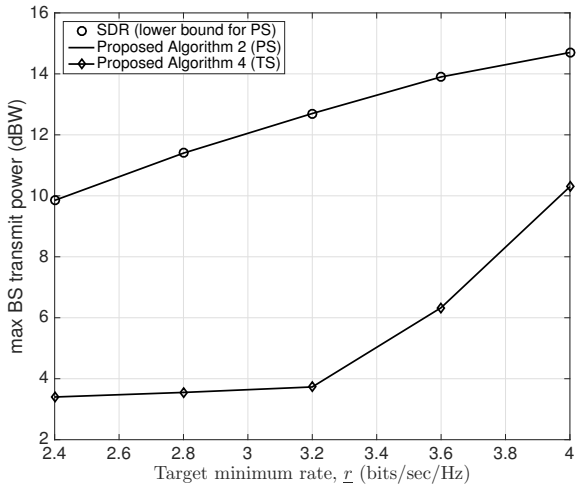


Fig. 7. Minimized maximum BS transmit power for $M = 5$.

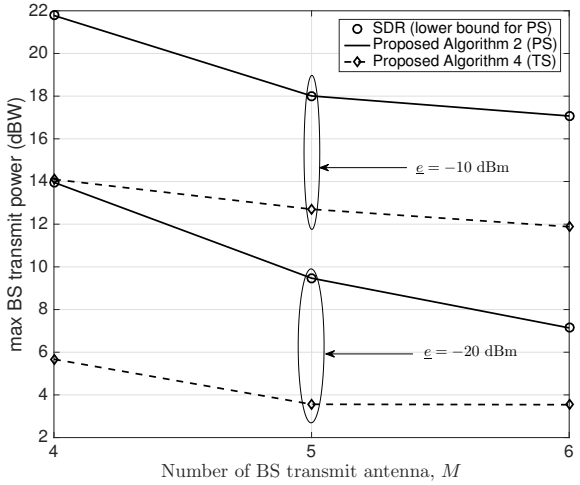


Fig. 8. Minimized maximum BS transmit power for $\underline{r} = 2.31$ bits/sec/Hz (i.e., $\underline{\gamma} = 6$ dB) and $\underline{e} = \{-20, -10\}$ dBm.

TABLE I
COMPLEXITY ANALYSIS FOR ALG. 1, SDR APPROACH AND [27] (TO SOLVE PROBLEM (7)), AND ALG. 3 (TO SOLVE PROBLEM (29))

| Algorithms | avg. # iter | scal var | lin cons | quad cons | SD cons |
|---|---|---|---|---|---|
| Alg. 1 (PS) | 11 | 60 | 24 | 16 | 0 |
| Algorithm of [27] (PS) | 26.5 | 132 | 40 | 0 | 36 |
| SDR approach (PS) | 17 | 132 | 40 | 24 | 12 |
| Alg. 3 (TS) | 6.8 | 97 | 25 | 20 | 0 |

mooth optimization algorithm of [27], the SDR method and Algorithm 3 are $\mathcal{O}\left(i_{\text{A1}}(M+1)^3K^3N^3(3KN+K+1)\right)$, $\mathcal{O}\left(i_{[26]}\left((M^2+M+2)KN/2\right)^3 (6KN+K+1)\right)$, $\mathcal{O}\left(i_{\text{SDR}}\left((M^2+M+2)KN/2\right)^3(6KN+K+1)\right)$ and $\mathcal{O}\big(i_{\text{A3}}\ (2KNM+1)^3(3KN\ +2K+3)\big)$, respectively [36]. Here, $i_{\text{A1}} = 11$ is the average number of times that QP (17) is solved by Algorithm 1; $i_{[26]} = 26.5$ is the average number of times that an SDP is solved by [27]; $i_{\text{SDR}} = 17$ is the average number of times that the feasibility (convex) SDR (A.1b)–(A.1f) is solved; and $i_{\text{A3}} = 6.8$ is the average number of times that QP (43) is solved by Algorithm 3. Note that the initialization (46) for Algorithm 3 requires 1.1 iterations on average. For the particular case of $M = 4, N = 4, K = 3$ and $P_k^{\max} = 16$ dBW, Table I shows the average number of iterations required ('avg. # iter.') as well as the numbers of scalar variables ('scal var'), linear constraints ('lin cons'), quadratic constraints ('quad cons') and semidefinite constraints ('SD cons') of the concerned algorithms. Clearly, Algorithms 1 and 3 are the most computationally efficient as they involve the smallest numbers of iterations, variables and constraints.

### *B. Results for Min-Max BS Power Optimization Problems* (19) *and* (30)

Algorithm 2 and the SDR approach are used to solve problem (19) whereas Algorithm 4 is to solve problem (30). Figs. 7 and 8 plot the minimized maximum BS transmit power for different values of the minimum rate $\underline{r}$ and BS transmit antenna number $M$. As expected, the BS transmit power requirement increases by setting higher target rates and decreases by using more BS antennas, respectively. In Fig. 8, we also evaluate the performance of the proposed algorithms for different values of the target minimum EH threshold $\underline{e} = \{-20, -10\}$ dBm. By increasing the target EH threshold from $\underline{e} = -20$ dBm to $\underline{e} = -10$ dBm, the required BS transmit power increases to meet the increased EH requirement. As can be observed, Algorithm 2 achieves the lower bound given by SDR under all the network settings considered. Furthermore, the transmit TS-based WIPT system by Algorithm 4 clearly outperforms the receive PS-based WIPT system by at least 3.5 dB in power.

Applying Algorithm 4 for the min-max BS power optimization problem (30), Fig. 9 plots the optimized value of the transmit TS ratio $\rho$ for different values of the target EH threshold $\underline{e}$ and the number of BS antennas $M = \{4, 5, 6\}$. Similar trends for the optimized TS ratio for Algorithm 3 in Fig. 5 can now be observed for Algorithm 4 in Fig. 9. Finally, Fig. 10 shows that Algorithm 2 quickly converges within 3 iterations to the theoretical lower bound obtained after solving the relaxed SDR (A.2a), (A.2b), (A.1e), (A.1f) [see AppendixA]. In this algorithm, each iteration corresponds to solving one SOCP (24). On the other hand, Algorithm 4 requires about 6 iterations to converge where each iteration

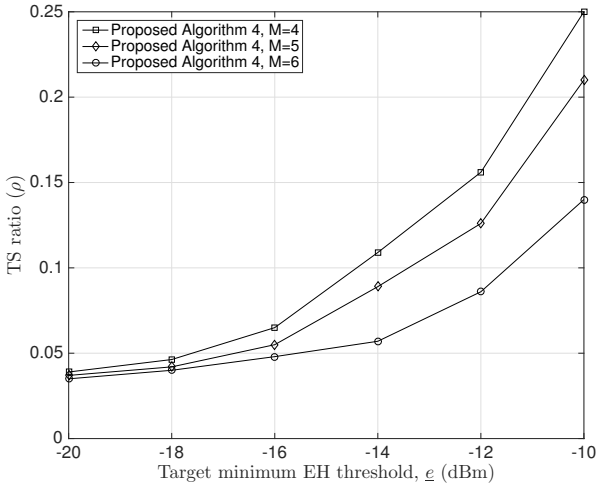


Fig. 9. Optimized TS ratio $\rho$ by Algorithm 4 for different numbers of BS antennas $M$ and $\underline{r} = 2.31$ bits/sec/Hz.

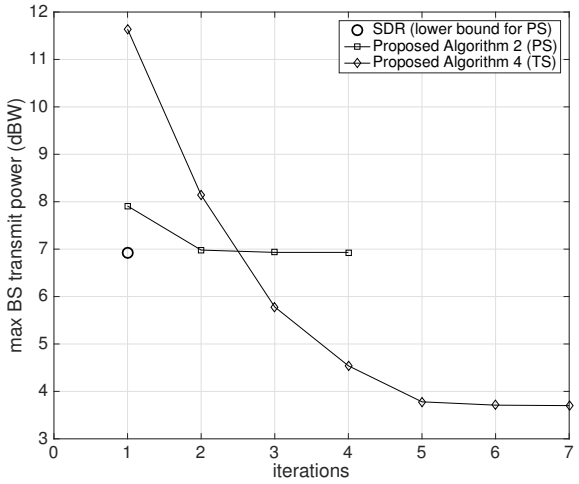


Fig. 10. Convergence of Algorithms 2 and 4 for $M = 5$ and $\underline{r} = 2.31$ bits/sec/Hz.

solves one QP (48).

The computational complexities of Algorithm 2, the SDR method and Algorithm 4 are $\mathcal{O}\left(i_{\mathrm{A2}}(M+2)^3K^3 N^3 4KN\right)$, $\mathcal{O}\left(\left((M^2+M+2)KN/2\right)^3 6KN\right)$ and $\mathcal{O}\left(i_{\mathrm{A4}}(2KNM+1)^3(4KN+K+2)\right)$, respectively [36]. Here $i_{\mathrm{A2}} = 3$ and $i_{\mathrm{A4}} = 6.99$ are the average number of iterations required for Algorithms 2 and 4 to converge. For the particular case of $M = 4, N = 4, K = 3$ and $\underline{r} = 2.316$ bit/sec/Hz, Table II shows the required number of variables and constraints, where 'SOC cons' denotes the required number of second-order cone constraints. Although Algorithm 4 for the transmit TS-based WIPT system requires more computational effort than Algorithm 2 for the receive PS-based WIPT system, the former system outperforms the latter system as previously shown in Figs. 7 and 8.

## V. Conclusions

In this paper, we have jointly designed the BS transmit beamformers with either the receive PS ratios or the transmit TS ratio for wireless energy harvesting multicell network. The design objectives include maximization of the minimum data rate among all UEs and minimization of the maximum BS transmit power. To solve the highly nonconvex problem formulations, we have proposed new iterative optimization algorithms of low computational complexity that are based on quadratic programming and second-order cone programming. Simulation results with practical parameters show that the algorithms converge quickly and that the transmit TS-based WIPT system outperforms the receive PS-based WIPT system. In the case of PS-based designs, the proposed algorithms tightly approach the theoretical bound in the considered numerical examples.

## Appendix A
## SDR-based Approach to solve Problems (7) and (19)

In the SDR-based approach, problem (7) in the beamforming vectors $\mathbf{w}_{k,n}$ is recast as the following problem in their outer products $\mathbf{W}_{k,n} \triangleq \mathbf{w}_{k,n}\mathbf{w}_{k,n}^H \succcurlyeq \mathbf{0}$:

$$\max_{\substack{\mathbf{W}_{k,n}\in\mathbb{C}^{M\times M},\\ \alpha_{k,n}\in(0,1),\gamma,\\ \forall\ k\in\mathcal{K},\ n\in\mathcal{N}_k}} \quad \gamma \tag{A.1a}$$

$$\text{s.t.} \quad \frac{1}{\gamma}\mathrm{Tr}\{\mathbf{H}_{k,k,n}\mathbf{W}_{k,n}\} - \sum_{\bar{n}\in\mathcal{N}_k\setminus\{n\}}\mathrm{Tr}\{\mathbf{H}_{k,k,n}\mathbf{W}_{k,\bar{n}}\} - \sum_{\bar{k}\in\mathcal{K}\setminus\{k\}}\sum_{\bar{n}\in\mathcal{N}_{\bar{k}}}\mathrm{Tr}\{\mathbf{H}_{\bar{k},k,n}\mathbf{W}_{\bar{k},\bar{n}}\} \geq \sigma_a^2 + \frac{\sigma_c^2}{\alpha_{k,n}},\ \forall k\in\mathcal{K}, n\in\mathcal{N}_k \tag{A.1b}$$

$$\sum_{n\in\mathcal{N}_k}\mathrm{Tr}\{\mathbf{W}_{k,n}\} \leq P_k^{\max},\ \forall k\in\mathcal{K} \tag{A.1c}$$

$$\sum_{k\in\mathcal{K}}\sum_{n\in\mathcal{N}_k}\mathrm{Tr}\{\mathbf{W}_{k,n}\} \leq P^{\max} \tag{A.1d}$$

$$\sum_{\bar{k}\in\mathcal{K}}\sum_{\bar{n}\in\mathcal{N}_{\bar{k}}}\mathrm{Tr}\{\mathbf{H}_{\bar{k},k,n}\mathbf{W}_{\bar{k},\bar{n}}\} \geq \frac{e_{k,n}^{\min}}{\zeta_{k,n}(1-\alpha_{k,n})} - \sigma_a^2,\ \forall k\in\mathcal{K}, n\in\mathcal{N}_k \tag{A.1e}$$

$$\mathbf{W}_{k,n} \succcurlyeq \mathbf{0},\ \forall k\in\mathcal{K}, n\in\mathcal{N}_k \tag{A.1f}$$

$$\mathrm{rank}(\mathbf{W}_{k,n}) = 1,\ \forall k\in\mathcal{K}, n\in\mathcal{N}_k. \tag{A.1g}$$

Let us denote $\mathbf{W} \triangleq [\mathbf{W}_{k,n}]_{k\in\mathcal{K},n\in\mathcal{N}_k}$. By fixing $\gamma$ and further ignoring the difficult rank-one constraint (A.1g), (A.1) is relaxed to the feasibility SDP (A.1b)–(A.1f). Because (A.1b) is the only constraint that involves $\gamma$ and it is monotonic in $\gamma$, the optimal value of $\gamma$ can be found via a bisection search in an outer loop. The optimization process is repeated until $(\mathbf{W}, \boldsymbol{\alpha}, \gamma)$ converges to $(\mathbf{W}^\star, \boldsymbol{\alpha}^\star, \gamma^\star)$, $\forall k \in \mathcal{K}, n \in \mathcal{N}_k$, in which case (A.1a)–(A.1f) is solved. The obtained solution by SDR approach is not guaranteed to be of rank one, i.e., $\mathrm{rank}(\mathbf{W}_{k,n}^\star) > 1$ is mostly observed. Thus, SDR-based

TABLE II
COMPLEXITY ANALYSIS FOR ALG. 2 AND SDR APPROACH (TO SOLVE PROBLEM (19)), AND ALG. 4 (TO SOLVE PROBLEM (30))

| Algorithms | avg. # iter | scal var | lin cons | quad cons | SD cons | SOC cons |
|---|---|---|---|---|---|---|
| Alg. 2 (PS) | 3 | 72 | 12 | 24 | 0 | 12 |
| SDR approach (PS) | 1 | 132 | 36 | 24 | 12 | 0 |
| Alg. 4 (TS) | 6.99 | 97 | 25 | 28 | 0 | 0 |

solution can serve as an upper bound for max-min rate problem (7) .

Similarly, problem (19) in beamforming vectors $\mathbf{w}_{k,n}$ is recast as the following rank-one constrained SDP in the outer products $\mathbf{W}_{k,n} \triangleq \mathbf{w}_{k,n}\mathbf{w}_{k,n}^H \succcurlyeq \mathbf{0},\ \forall k \in \mathcal{K}, n \in \mathcal{N}_k$:

$$\min_{\substack{\mathbf{W}_{k,n}\in\mathbb{C}^{M\times M},\\ \alpha_{k,n}\in(0,1),\\ \forall\ k\in\mathcal{K},\ n\in\mathcal{N}_k}} \max_{k\in\mathcal{K}} \sum_{n\in\mathcal{N}_k} \mathrm{Tr}\{\mathbf{W}_{k,n}\} \tag{A.2a}$$

$$\text{s.t.}\quad \mathrm{Tr}\{\mathbf{H}_{k,k,n}\mathbf{W}_{k,n}\} \geq \gamma_{k,n}^{\min}\left(\sum_{\bar{n}\in\mathcal{N}_k\setminus\{n\}} \mathrm{Tr}\{\mathbf{H}_{k,k,n}\mathbf{W}_{k,\bar{n}}\} + \sum_{\bar{k}\in\mathcal{K}\setminus\{k\}}\sum_{\bar{n}\in\mathcal{N}_{\bar{k}}} \mathrm{Tr}\{\mathbf{H}_{\bar{k},k,n}\mathbf{W}_{\bar{k},\bar{n}}\} + \sigma_a^2 + \frac{\sigma_c^2}{\alpha_{k,n}}\right),\quad \forall k \in \mathcal{K}, n \in \mathcal{N}_k \tag{A.2b}$$

$$(\text{A.1e}), (\text{A.1f}), (\text{A.1g}). \tag{A.2c}$$

By ignoring the rank-one constraint (A.1g), the optimal solution $\sum_{k\in\mathcal{K}}\sum_{n\in\mathcal{N}_k} \mathrm{Tr}\{\mathbf{W}_{k,n}^\star\}$ of the SDR formed by (A.2a), (A.2b), (A.1e), (A.1f) provides a lower bound of the actual optimal value of problem (19).

## REFERENCES


[1] J. Andrews, S. Buzzi, W. Choi, S. Hanly, A. Lozano, A. Soong, and J. Zhang, "What will 5G be?" *IEEE J. Sel. Areas Commun.*, vol. 32, no. 6, pp. 1065–1082, Jun. 2014.

[2] L. R. Varshney, "Transporting information and energy simultaneously," in *Proc. IEEE ISIT*, Toronto, Canada, Jul. 2008, pp. 1612–1616.

[3] A. A. Nasir, X. Zhou, S. Durrani, and R. A. Kennedy, "Relaying protocols for wireless energy harvesting and information processing," *IEEE Trans. Wireless Commun.*, vol. 12, no. 7, pp. 3622–3636, Jul. 2013.

[4] K. Huang and V. K. N. Lau, "Enabling wireless power transfer in cellular networks: Architecture, modeling and deployment," *IEEE Trans. Wireless Commun.*, vol. 13, no. 2, pp. 902–912, Feb. 2014.

[5] X. Lu, P. Wang, D. Niyato, D. I. Kim, and Z. Han, "Wireless networks with RF energy harvesting: A contemporary survey," *IEEE Commun. Surveys Tuts.*, vol. 17, pp. 757–789, 2015.

[6] K. Huang and X. Zhou, "Cutting last wires for mobile communications by microwave power transfer," *IEEE Commun. Mag.*, vol. 53, Jun. 2015.

[7] J. Huang, H. Zhang, W. Xu, and H. Zhang, "Grouping based inter-cell interference coordination in LTE-A dense small-cell networks," in *Proc. IEEE MAPE*, Oct. 2013, pp. 78–83.

[8] H. Morosa, H. Harada, A. Morimoto, S. Nasata, H. Ishii, and Y. Okumura, "Cell identification performance based on hierarchical synchronization channels in dense small cell environment," in *Proc. IEEE SPAWC*, Jun. 2013, pp. 734–738.

[9] W. Liu, X. Zhou, S. Durrani, and P. Popovski, "SWIPT with practical modulation and rf energy harvesting sensitivity," in *Proc IEEE ICC*, May 2016, pp. 1–7.

[10] Z. Ding, C. Zhong, D. W. Kwan, M. Peng, H. A. Suraweera, R. Schober, and H. V. Poor, "Application of smart antenna technologies in simultaneous wireless information and power transfer," *IEEE Commun. Magazine*, vol. 53, no. 4, pp. 86–93, 2015.

[11] Z. Ding, S. M. Perlaza, I. Esnaola, and H. V. Poor, "Power allocation strategies in energy harvesting wireless cooperative networks," *IEEE Trans. Wireless Commun.*, vol. 13, no. 2, pp. 846–860, Feb. 2014. [Online]. Available: http://arxiv.org/abs/1307.1630

[12] Z. Ding, I. Krikidis, B. Sharif, and H. Poor, "Wireless information and power transfer in cooperative networks with spatially random relays," *IEEE Trans. Wireless Commun.*, vol. 13, no. 8, pp. 4440–4453, Aug. 2014.

[13] Y. Liu, Z. Ding, M. Elkashlan, and H. V. Poor, "Cooperative non-orthogonal multiple access with simultaneous wireless information and power transfer," *IEEE J. Selec. Areas Commun.*, vol. 34, no. 4, pp. 938–953, Apr. 2016.

[14] H. Dahrouj and W. Yu, "Coordinated beamforming for the multicell multi-antenna wireless system," *IEEE Trans. Wireless Commun.*, vol. 9, no. 5, pp. 1748–1759, May 2010.

[15] S. He, Y. Huang, L. Yang, A. Nallanathan, and P. Liu, "A multi-cell beamforming design by uplink-downlink max-min SINR duality," *IEEE Trans. Wireless Commun.*, vol. 11, no. 8, pp. 2858–2867, Aug. 2012.

[16] H. Pennanen, A. Tolli, and M. Latva-aho, "Multi-cell beamforming with decentralized coordination in cognitive and cellular networks," *IEEE Trans. Signal Process.*, vol. 62, no. 2, pp. 295–308, Jan. 2014.

[17] E. Che and H. D. Tuan, "Sum-rate based coordinated beamforming in multicell multi-antenna wireless networks," *IEEE Commun. Letters*, vol. 18, no. 6, pp. 1019–1022, 2014.

[18] E. Che, H. D. Tuan, H. H. M. Tam, and H. H. Nguyen, "Maximisation of sum rate in cognitive multi-cell wireless networks with QoS constraints," in *Proc. IEEE ICSPCS*, 2014.

[19] Y. Huang and D. P. Palomar, "Rank constrained separable semidefinite program with applications to optimal beamforming," *IEEE Trans. Signal Process.*, vol. 2, no. 5, pp. 664–678, Feb 2010.

[20] Z. Zhu, Z. Wang, X. Gui, and X. Gao, "Robust downlink beamforming and power splitting design in multiuser MISO SWIPT system," in *Proc. IEEE ICCC*, Oct. 2014, pp. 271–275.

[21] Q. Shi, L. Liu, W. Xu, and R. Zhang, "Joint transmit beamforming and receive power splitting for MISO SWIPT systems," *IEEE Trans. Wireless Commun.*, vol. 13, no. 6, pp. 3269–3280, Jun. 2014.

[22] M. Khandaker and K.-K. Wong, "SWIPT in MISO multicasting systems," *IEEE Wireless Commun. Lett.*, vol. 3, no. 3, pp. 277–280, Jun. 2014.

[23] Q. Shi, W. Xu, T.-H. Chang, Y. Wang, and E. Song, "Joint beamforming and power splitting for MISO interference channel with SWIPT: An SOCP relaxation and decentralized algorithm," *IEEE Trans. Signal Process.*, vol. 62, no. 23, pp. 6194–6208, Dec. 2014.

[24] S. Timotheou, I. Krikidis, G. Zheng, and B. Ottersten, "Beamforming for MISO interference channels with QoS and RF energy transfer," *IEEE Trans. Wireless Commun.*, vol. 13, no. 5, pp. 2646–2658, May 2014.

[25] A. H. Phan, H. D. Tuan, H. H. Kha, and D. T. Ngo, "Nonsmooth optimization for efficient beamforming in cognitive radio multicast transmission," *IEEE Trans. Signal Process.*, vol. 60, no. 6, pp. 2941–2951, Jun. 2012.

[26] U. Rashid, H. D. Tuan, and H. H. Nguyen, "Relay beamforming designs in multi-user wireless relay networks based on throughput maximin optimization," *IEEE Trans. Commun.*, vol. 51, no. 5, pp. 1734–1749, 2013.

[27] A. A. Nasir, D. T. Ngo, H. D. Tuan, and S. Durrani, "Iterative optimization for max-min SINR in dense small-cell multiuser MISO SWIPT system," in *Proc. IEEE Global Conference on Signal Processing (GlobalSIP)*, 2015.

[28] H. Zhang, K. Song, Y. Huang, and L. Yang, "Energy harvesting balancing technique for robust beamforming in multiuser MISO SWIPT system," in *Proc. IEEE WCSP*, Oct. 2013, pp. 1–5.
[29] A. H. Phan, H. D. Tuan, H. H. Kha, and H. H. Nguyen, "Beamforming optimization in multi-user amplify-and-forward wireless relay networks," *IEEE Trans. Wireless Commun.*, vol. 11, no. 4, pp. 1510–1520, Apr. 2012.
[30] A. H. Phan, H. D. Tuan, and H. H. Kha, "D.C. iterations for SINR maximin multicasting in cognitive radio," in *Proc. IEEE ICSPCS*, 2012.
[31] H. H. Kha, H. D. Tuan, and H. H. Nguyen, "Fast global optimal power allocation in wireless networks by local D.C. programming," *IEEE Trans. Wireless Commun.*, vol. 11, no. 2, pp. 510–515, Feb. 2012.
[32] A. Wiesel, Y. Eldar, and S. Shamai, "Linear precoding via conic optimization for fixed MIMO receivers," *IEEE Trans. Signal Processing*, vol. 54, no. 1, pp. 161–176, Jan. 2006.
[33] H. Tuy, *Convex Analysis and Global Optimization*. Kluwer Academic, 2001.
[34] B. R. Marks and G. P. Wright, "A general inner approximation algorithm for nonconvex mathematical programs," *Operation Research*, vol. 26, no. 4, pp. 681–683, 1978.
[35] M. Grant and S. Boyd, "CVX: Matlab software for disciplined convex programming, version 2.1," http://cvxr.com/cvx, Mar. 2014.
[36] D. Peaucelle, D. Henrion, and Y. Labit, "Users guide for SeDuMi interface 1.03," 2002. [Online]. Available: http://homepages.laas.fr/peaucell/software/sdmguide.pdf

**Ali Arshad Nasir** (S09-M13) is an Assistant Professor in the Department of Electrical Engineering, King Fahd University of Petroleum and Minerals (KFUPM), Dhahran, KSA. Previously, he held the position of Assistant Professor in the School of Electrical Engineering and Computer Science (SEECS) at National University of Sciences & Technology (NUST), Paksitan, from 2015-2016. He received his Ph.D. in telecommunications engineering from the Australian National University (ANU), Australia in 2013 and worked there as a Research Fellow from 2012-2015. His research interests are in the area of signal processing in wireless communication systems. He is an Associate Editor for IEEE Canadian Journal of Electrical and Computer Engineering.

**Hoang Duong Tuan** received the Diploma (Hons.) and Ph.D. degrees in applied mathematics from Odessa State University, Ukraine, in 1987 and 1991, respectively. He spent nine academic years in Japan as an Assistant Professor in the Department of Electronic-Mechanical Engineering, Nagoya University, from 1994 to 1999, and then as an Associate Professor in the Department of Electrical and Computer Engineering, Toyota Technological Institute, Nagoya, from 1999 to 2003. He was a Professor with the School of Electrical Engineering and Telecommunications, University of New South Wales, from 2003 to 2011. He is currently a Professor with the Centre for Health Technologies, University of Technology Sydney. He has been involved in research with the areas of optimization, control, signal processing, wireless communication, and biomedical engineering for more than 20 years.

**Duy Trong Ngo** (S'08-M'15) received the B.Eng. (with First-class Honours and the University Medal) degree in telecommunication engineering from The University of New South Wales, Australia in 2007, the M.Sc. degree in electrical engineering (communication) from University of Alberta, Canada in 2009, and the Ph.D. degree in electrical engineering from McGill University, Canada in 2013.

Since 2013, he has been a Lecturer with the School of Electrical Engineering and Computing, The University of Newcastle, Australia, where he currently leads the research effort in design and optimization for 5G wireless communications networks.

In 2013, Dr. Ngo was awarded two prestigious Postdoctoral Fellowships from the Natural Sciences and Engineering Research Council of Canada and the Fonds de recherche du Québec – Nature et technologies. At The University of Newcastle, he received the 2015 Vice-Chancellor's Award for Research and Innovation Excellence and the 2015 Pro Vice-Chancellor's Award for Research Excellence in the Faculty of Engineering and Built Environment.

**Trung Q. Duong** (S'05, M'12, SM'13) received his Ph.D. degree in Telecommunications Systems from Blekinge Institute of Technology (BTH), Sweden in 2012. Since 2013, he has joined Queen's University Belfast, UK as a Lecturer (Assistant Professor). His current research interests include physical layer security, energy-harvesting communications, cognitive relay networks. He is the author or co-author of more than 220 technical papers published in scientific journals (110 articles) and presented at international conferences (110 papers).

Dr. Duong currently serves as an Editor for the IEEE TRANSACTIONS ON WIRELESS COMMUNICATIONS, IEEE TRANSACTIONS ON COMMUNICATIONS, IEEE COMMUNICATIONS LETTERS, IET COMMUNICATIONS. He was a Editor of WILEY TRANSACTIONS ON EMERGING TELECOMMUNICATIONS TECHNOLOGIES, ELECTRONICS LETTERS and has also served as the Guest Editor of the special issue on some major journals including IEEE JOURNAL IN SELECTED AREAS ON COMMUNICATIONS, IET COMMUNICATIONS, IEEE ACCESS, IEEE WIRELESS COMMUNICATIONS MAGAZINE, IEEE COMMUNICATIONS MAGAZINE, EURASIP JOURNAL ON WIRELESS COMMUNICATIONS AND NETWORKING, EURASIP JOURNAL ON ADVANCES SIGNAL PROCESSING. He was awarded the Best Paper Award at the IEEE Vehicular Technology Conference (VTC-Spring) in 2013, IEEE International Conference on Communications (ICC) 2014. He is the recipient of prestigious Royal Academy of Engineering Research Fellowship (2016-2021).

**Vincent Poor** (S72, M77, SM82, F87) received the Ph.D. degree in EECS from Princeton University in 1977. From 1977 until 1990, he was on the faculty of the University of Illinois at Urbana-Champaign. Since 1990 he has been on the faculty at Princeton, where he is the Michael Henry Strater University Professor of Electrical Engineering. From 2006 till 2016, he served as Dean of Princetons School of Engineering and Applied Science. Dr. Poors research interests are in the areas of statistical signal processing, stochastic analysis and information theory, and their applications in wireless networks and related fields. Among his publications in these areas is the recent book Mechanisms and Games for Dynamic Spectrum Allocation (Cambridge University Press, 2014).

Dr. Poor is a member of the National Academy of Engineering and the National Academy of Sciences, and a foreign member of the Royal Society. He is also a Fellow of the American Academy of Arts and Sciences and the National Academy of Inventors, and of other national and international academies. He received the Technical Achievement and Society Awards of the IEEE Signal Processing Society in 2007 and 2011, respectively. Recent recognition of his work includes the 2014 URSI Booker Gold Medal, the 2015 EURASIP Athanasios Papoulis Award, the 2016 John Fritz Medal, and honorary doctorates from Aalborg University, Aalto University, HKUST and the University of Edinburgh.